



Transient behaviour and helium recovery in the LHC cryogenic system following magnet resistive transitions

M.Chorowski / LHC-ACR

Keywords: magnet quench, helium enthalpy, recovery system

Summary

The aim of the study is to determine helium parameters in LHC cryogenic system after a machine quench. Then the LHC quenches are classified from their cryogenic consequences. Finally a configuration of helium recovery system elements and procedures are proposed.

1. Resistive transition of LHC magnets.

An energy stored in a LHC half-cell and relieved during a resistive transition ("quench") may be as high as 23 MJ [1]. After a quench the stored energy is dissipated in the cold mass within a few tenths of a second. A fraction of this energy is transferred to the helium inside the porous windings and in the annular space around the beam tubes, causing expansion and axial flow to the end volumes of the helium vessel. Helium is finally discharged to the helium recovery system through a quench relief valve at each end of the half-cell.

2. The LHC helium recovery system.

The task of the system is recovery of the helium inventory and its refrigeration capacity after a machine quench. A general scheme of the helium recovery system for one LHC sector is shown in figure 1. The system consists of the following nodes:

- a vacuum insulated line D of a length equal to about 3400 m per sector, connected through quench relief valves with the LHC half-cells in number up to 54 per sector,

- an uninsulated vertical line (length ranging from 42 to 145 m, depending on the access point), connecting line D with medium-pressure gas storage tanks,
- medium-pressure gas storage tanks,
- piping and auxiliaries interconnecting the system with the sector refrigerator.

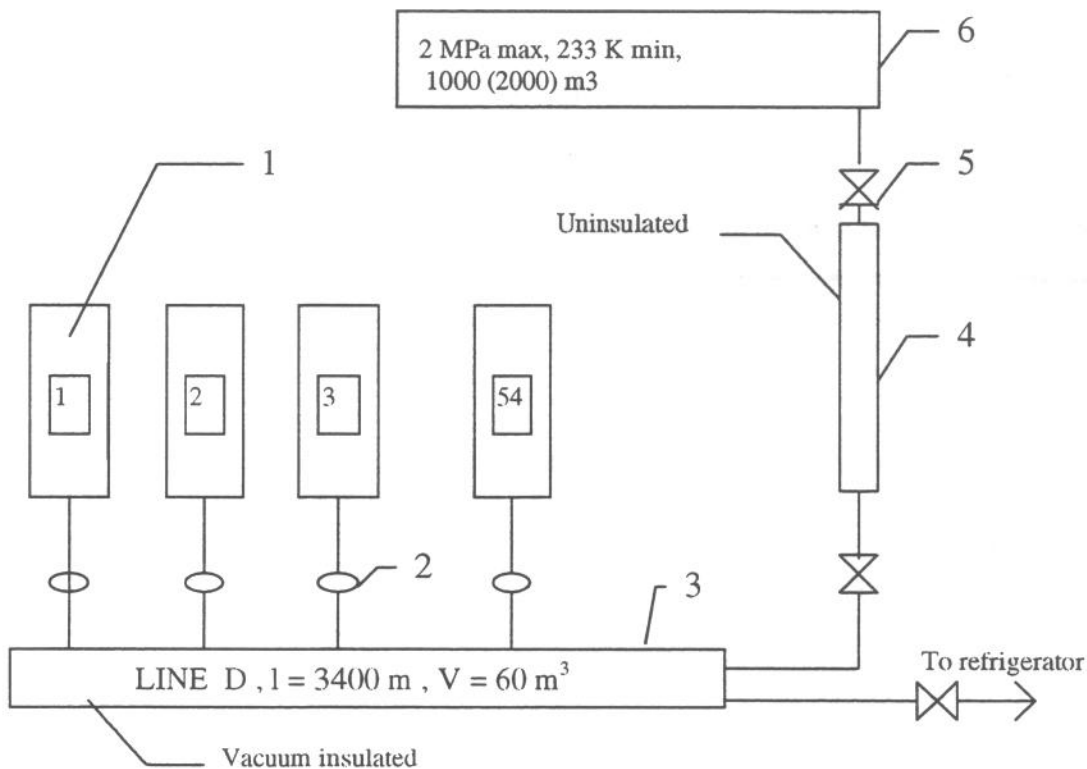


Fig.1. Helium recovery system, schema for one sector, 1 - cryogenic half cells (in number 46 to 54 per sector), 2 - quench relief valves, 3 - vacuum insulated line D, 4 - uninsulated vertical line (42 to 145 m long, depending on the access point), 5 - valves, 6 - medium pressure gas tanks.

Helium recovery also implies specific procedures that should follow a quench, in order to save:

- helium inventory,
- helium refrigeration capability (exergy).

3. Lumped parameter approach to the recovery system.

A basic assumption is that the lumped-parameter approach is adequate. A node represents an individual system element. Within a node (e.g. line D, or medium

pressure gas tank), spatial variations of density, temperature and pressure are assumed to be negligible. For each node of the helium recovery system, the following equation of energy balance can be written

$$dU = dQ + \sum_i (h_i + \frac{w_i^2}{2} + l_i g) dM_i \quad , \quad (1)$$

where:

dU -energy change of the system element (node) [J],

dQ - heat transferred to a node [J],

h_i -enthalpy of the i -th stream of helium leaving or entering a node [J/kg],

g - acceleration of gravity [9.81 m/s²],

l - height above the tunnel level [m],

w - velocity of the i -th stream [m/s],

dM_i - change of the mass of helium in a node due to the i -th flow [kg].

4. Enthalpy of helium leaving the cold mass after the quench.

The enthalpy of helium leaving the cold mass after a quench is a basic input for any further calculations. The most reliable approach seems to be using experimental data from the prototype magnet string [2], in order to calculate:

- the average enthalpy of helium leaving the cold mass - from the string energy balance,
- the enthalpy flow of helium leaving the cold mass - from measurements of helium pressure and temperature in the string cold mass, pressure in line D and k_v coefficient of the quench relief valve.

4.1. The prototype magnet string energy balance.

The string is a fully working model of the future LHC half-cell apart from the particle beams. The simplified string cryogenic flow scheme is shown in figure 2. The energy stored in a superconducting magnets E_{Coil} , and dissipated after a quench, finally ends up as:

- energy accumulated as heat in magnets cold masses - $\Delta E_{Magnets}$
- energy transferred to helium which did not leave the cold mass - $\Delta E_{He-cold-mass}$
- energy transferred to helium expelled from the cold mass - $\Delta E_{He-expelled}$

The string energy balance equation is thus:

$$E_{Coil} = \Delta E_{Magnets} + \Delta E_{He-cold-mass} + \Delta E_{He-expelled} \quad , \quad (2)$$

and energy transferred to the helium expelled from a cold mass is

$$\Delta E_{He-expelled} = E_{Coil} - (\Delta E_{Magnets} + \Delta E_{He-cold-mass}) \quad . \quad (2a)$$

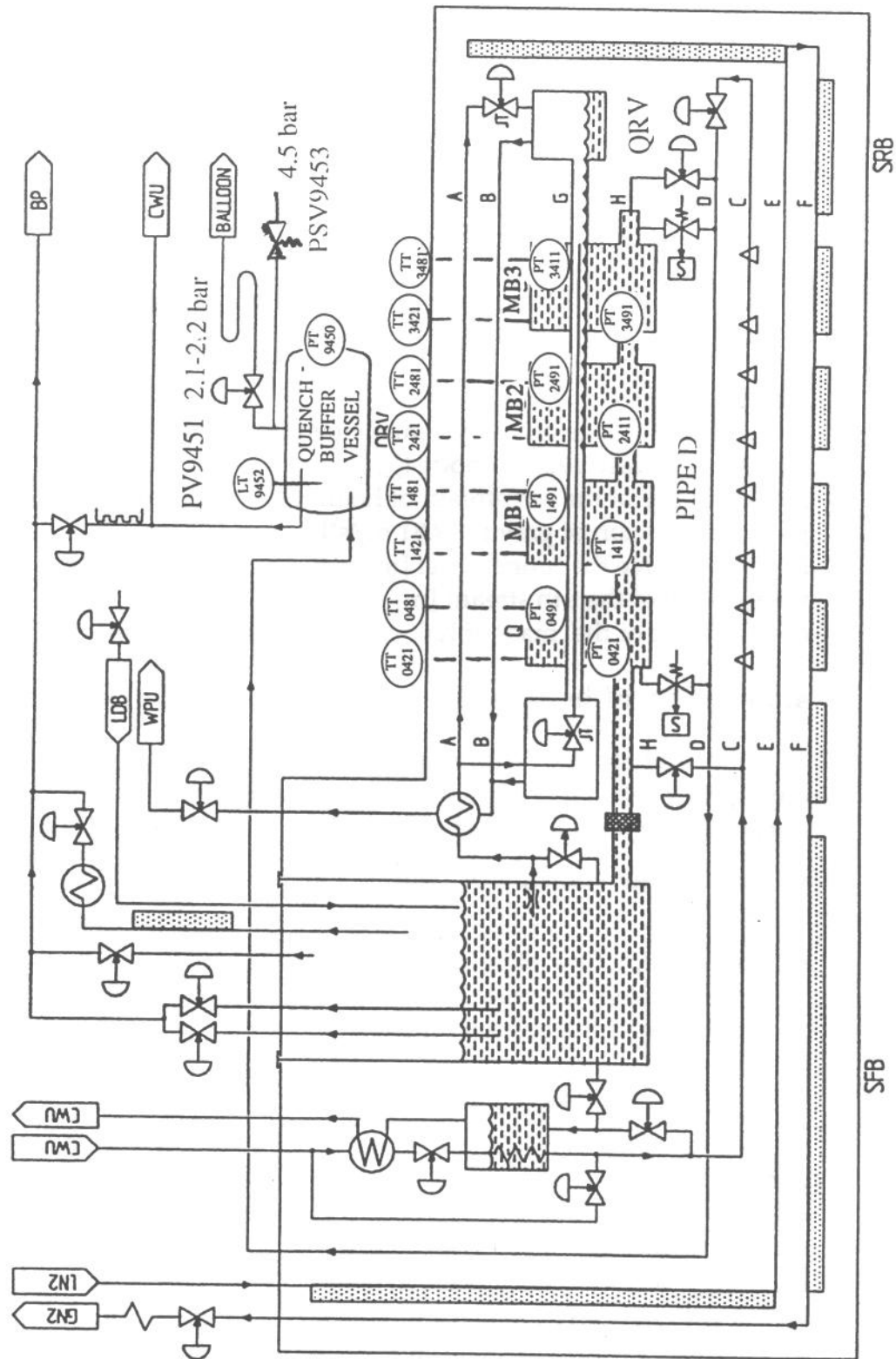


Fig. 2. String simplified cryogenic flow scheme [2], TT - temperature sensors, PT - pressure sensors, LT - level sensor, QRV, PV, PSV - valves

E_{Coil} calculation.

The following string runs were used as data sources: 613, 626, 633, 635, 638, 651, 653, 675, 677, 692, 842. In each case the current was equal to 13.1 kA and the corresponding stored energy E_{Coil} was equal to 15.273 MJ* (string self-inductance is equal to 178 [mH]).

Helium was expelled from the cold mass through a quench relief valve located at the upper part of string return box, close to the dipole three. The second quench relief valve, located close to the quadrupole, remained closed. The above configuration has matched in the best way the LHC future quench relief valves layout [3].

$\Delta E_{\text{Magnets}}$ calculation.

A typical evolution of cold mass temperatures after a 13.1 kA quench is shown in figure 3.

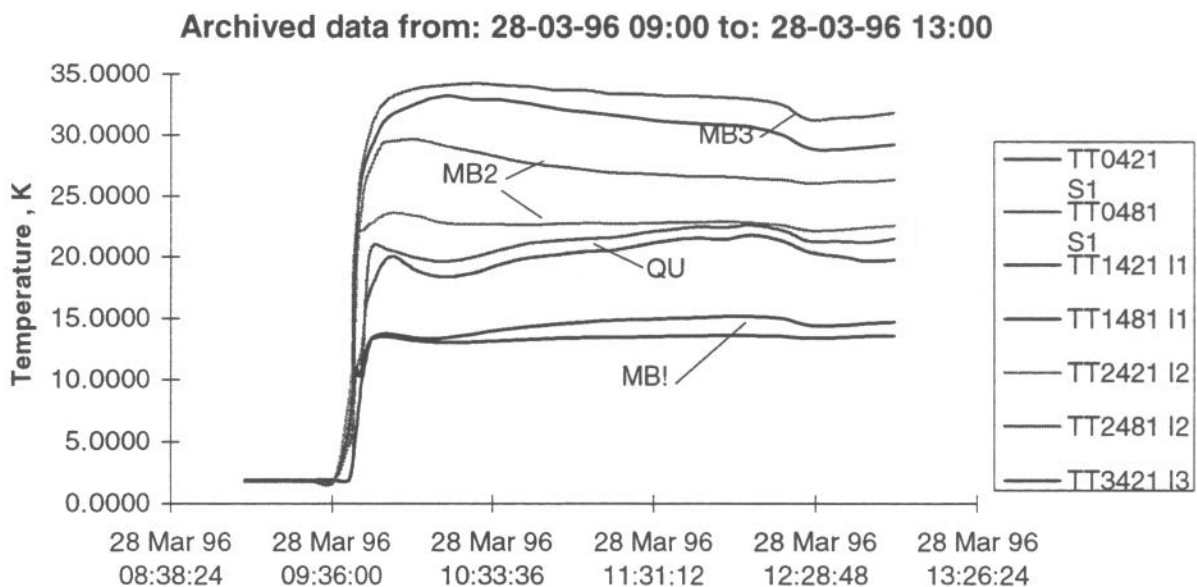


Fig.3. Temperature of the magnets after a quench, RUN 677, current 13.1 kA. See figure 2 for position of temperature measurements.

The temperature of the cold mass stabilize a few minutes after the quench. Then the maximal cold mass temperatures can be measured. The temperature of each cold mass is measured in two points (e.g. TT1421 and TT1481 for dipole 1). These temperatures are slightly different. The final cold mass temperature was taken as the

* The string E_{Coil} energy is lower than the corresponding LHC half-cell energy. But the energy ratio (23MJ/15MJ) is similar to the dipole length ratio (14.2m/9.7m) and an energy increase will be accompanied by a proportional increase in cold mass. Hence the energy distribution after a quench should be in both cases similar.

higher of the two measured for the each cold mass. Then the energy accumulated in each cold mass was calculated and summed altogether (3)

$$\Delta E_{Magnets} = \sum_{i=1}^3 M_{D_i} \int_{1.8}^{\vartheta_{D_i}} c_{D_i} d\vartheta + M_Q \int_{1.8}^{\vartheta_Q} c_Q d\vartheta, \quad (3)$$

where: D_i - dipole, Q - quadrupole, ϑ - temperature, c , M - magnet heat capacity and mass [4].

Because of the differences in final cold mass temperatures observed even for quenches characterised by the same operating current, averaging was used to estimate $\Delta E_{Magnets}$. A mean value of thermal energy $\Delta E_{Magnets}$ transferred to the magnets cold mass is equal to 9779 kJ, with a standard deviation 287 kJ (3 % of the mean value), as can be seen in figure 4.

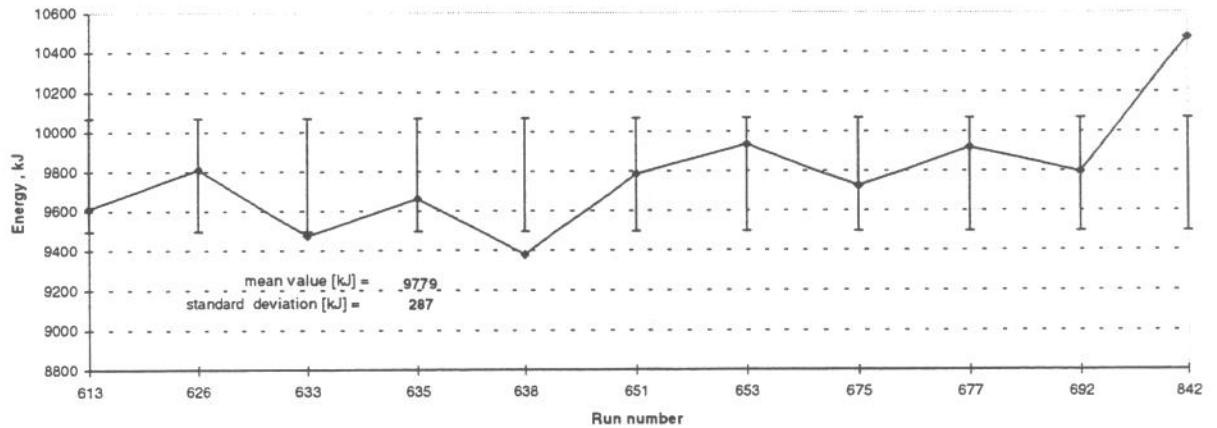


Fig. 4. Thermal energy accumulated in the string cold mass after a quench at 13.1 kA.

$\Delta E_{He-cold-mass}$ calculation.

Energy transferred to helium left in the cold mass is equal to:

$$\Delta E_{He-cryostat} = M_{He-cold-mass} \cdot \Delta h_{He-cold-mass}, \quad (4)$$

$$\Delta h_{He-cold-mass} = h_{final} - h_{initial} \quad (4a)$$

Helium enthalpies $h_{initial}$ and h_{final} were calculated for average temperatures and pressures measured in the string cold mass before and after a quench.

Final energy distribution.

Figures 5 and 6 show the final distribution of energy, i.e. that obtained approximately 60 minutes after a quench at 13.1 kA.

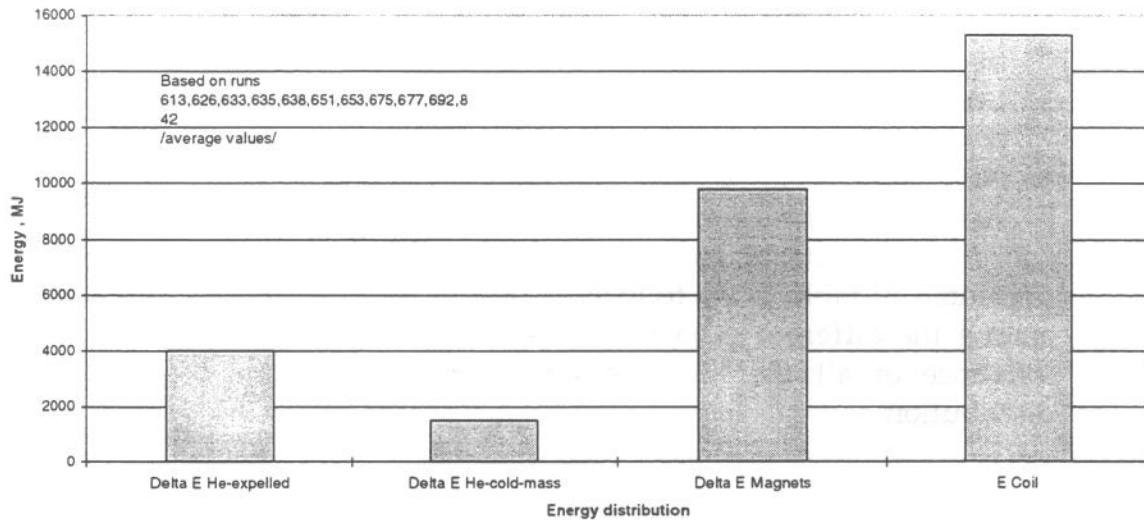


Fig.5. Final energy distribution after a 13.1 kA quench - absolute values.

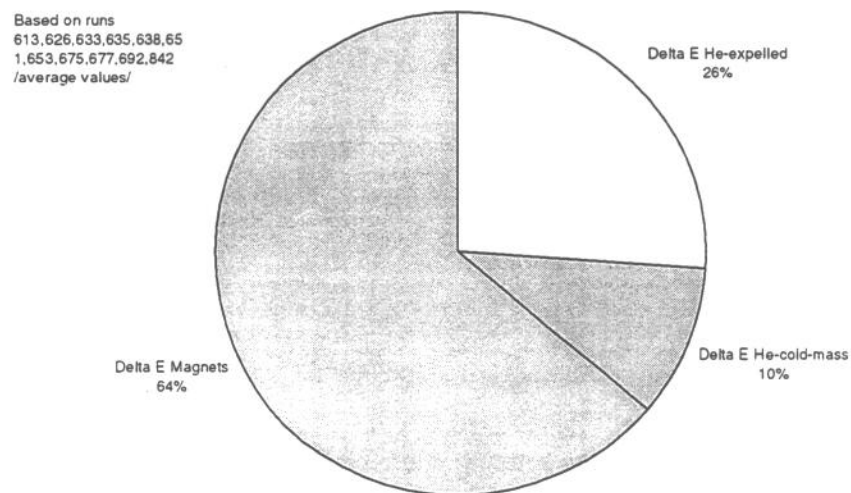


Fig.6. Final energy distribution after a 13.1 kA quench - relative values.

Helium expelled to line D absorbs 26% of the E_{Coil} energy after a 13.1 kA quench. One observes a highly uneven $\Delta E_{Magnets}$ energy partition among the different dipoles, and after averaging experimental data one gets: $E_{Dipole1} : E_{Dipole2} : E_{Dipole3} = 1 : 7 : 11$. Figure 7 illustrates the distribution of $E_{Magnets}$ among the different magnets. The major part (54%) of the thermal energy transferred to the cold mass is accumulated in dipole 3. There are several possible causes for this phenomenon:

1. Different electrical features of the dipoles - e.g. the RRR values of the coils - see appendix 1.
2. Differences in heat transfer coefficient between the cold mass and helium along the string, due to helium density stratification - see appendix 2.
3. Convective cooling of dipole 1 due to the string slope and helium density stratification.
4. Non-equal helium distribution along the string.
5. Accuracy in the estimation of the final cold mass temperatures.

The results of analysis of the possible magnitude of the above effects are presented in table 1. As follows of table 1 an observed uneven energy distribution among the different dipoles is not a result of a single cause. Only a simultaneous influence of all the analysed effects may justify the observed ratio in energy distribution.

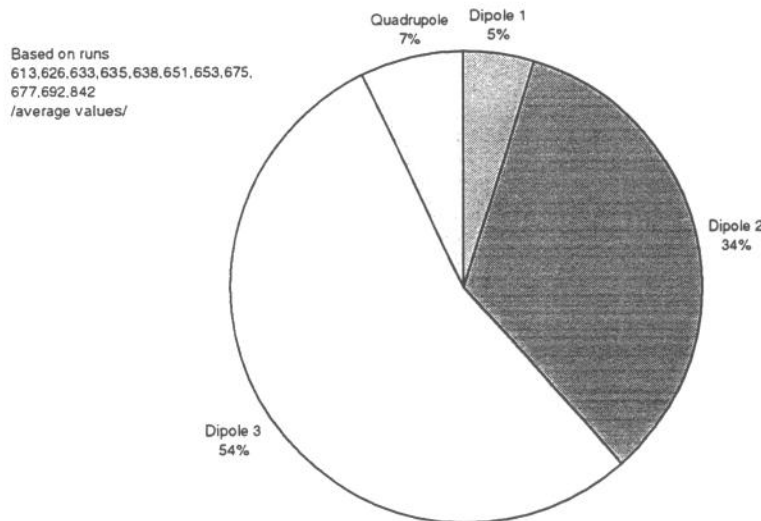


Fig. 7. Energy distribution among the STRING magnets after a 13.1 kA quench - relative values.

Calculation of an average enthalpy h_{He} of helium leaving the cold mass.

With a known amount of energy transferred to helium expelled from the cold mass, its average enthalpy \bar{h}_{He} can be calculated as follows:

$$\bar{h}_{He} = (h_{He-initial} \Delta M_{He-expelled} + \Delta E_{He-expelled}) / \Delta M_{He-expelled} , \quad (5)$$

where:

$h_{He-initial} = 1864$ J/kg - helium enthalpy for a 1 bar pressure and 1.9 K temperature,
 $\Delta M_{He-expelled} = 120$ kg of helium for each quench (initial amount of helium inside the string is 126.5 kg, an average amount of 6.2 kg is left inside after a quench).

Table 1. Possible effects causing uneven energy dissipation in the different dipoles of the string.

Nr.	Effect	Estimated gain of the effect $E_{Dip1}:E_{Dip2}:E_{Dip3}$	Remarks
1	Differences in RRR values of the coils	1 : 1.1 : 1.3	The lack of major differences in dipoles electrical features was confirmed by their similar behaviour on the test bench. Final dipole temperatures measured 15 minutes after a 13 kA quench on the test bench did not differ more than 1 K [3].
2	Different values of heat transfer coefficients	1 : 2.1 : 2.3	Helium density stratification along the string influences the heat transfer coefficients and hence: dipole 1 is more efficiently cooled than dipole 2, and dipole 2 is more efficiently cooled than dipole 3. The estimation of the effect gain is based on run 633.
3	Convective cooling of the dipole1	1 : 1.1 : 1.2	In result of density stratification due to the string slope, a convective flow of helium is possible. An integrated helium flow from dipole 3 to dipole 1 may be equal to 14 kg and the corresponding integrated additional cooling power of dipole 1 - 180 kJ (estimation based on run 633).
4	Non-equal helium distribution along the string	1 : 1.4 : 1.6	The distribution of helium along the string is not a constant function of its length. The majority of helium stays close to the quadrupole and dipole 1 (ca 500 dm ³), while dipole 2 is cooled by approximately 220 dm ³ and dipole 3 by 130 dm ³ .
5	Accuracy in final magnets temperatures estimations	1 : 1.1 : 1.2	Final magnets temperatures are measured about 60 minutes after a quench but even then they are characterised by some low frequency fluctuations (see fig.3). Hence 1 K accuracy in final temperature estimation seems a reasonable number. Because of non-linear dependence of cold mass heat capacity on temperature, the effect may be gained in a significant way.
6	All effects	1 : 4 : 7	All effects acting simultaneously, superposition assumed, final gain may be higher because of non-linearity.

Figure 8 shows a statistical analysis of an average enthalpy of helium expelled from the cold mass. An average helium enthalpy is 33.29 J/g and its standard deviation is 2.36 J/g. Hence we can expect the helium enthalpy to belong to the range 31 - 36 J/g.

4.2. Enthalpy flow of helium leaving the cold mass.

Enthalpy of helium leaving the cold mass was calculated as a function of helium temperature and pressure. Helium temperature was taken as an average value

of the following sensors: TT1481, TT2421, TT2481, TT3421. Helium pressure was taken as an mean value of sensors: PT1491, PT2411, PT2491, PT3411. The time evolution of enthalpy h_{He} of helium leaving the cold mass after a quench is shown in figure 9.

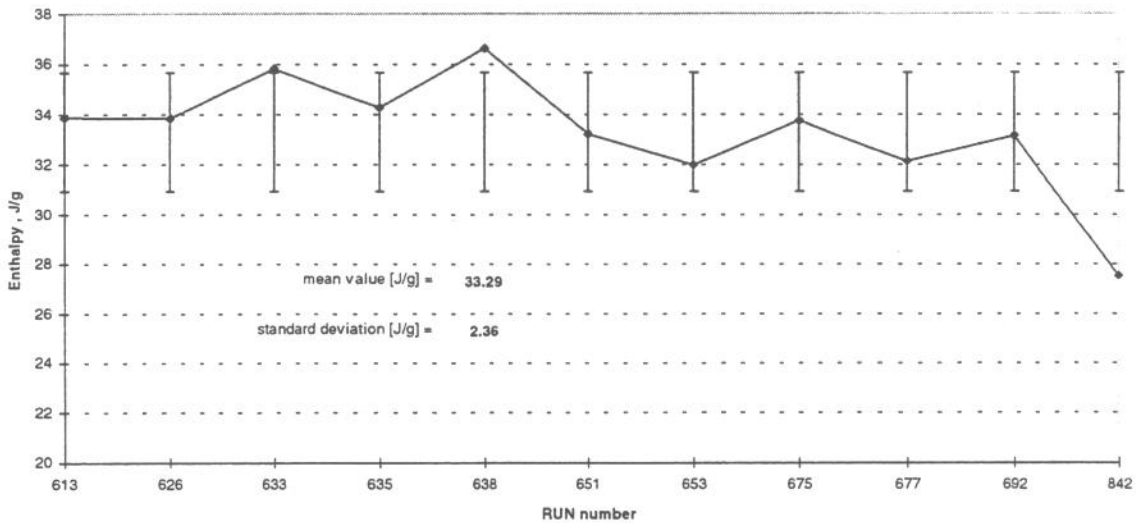


Fig. 8. Average enthalpy of helium leaving the cold mass after a 13.1 kA quench.

To calculate the discharged helium mass flow the following formula was used:

$$\dot{M} = \frac{\sqrt{998.5}}{3600} \cdot k_v \sqrt{\Delta p \rho} \quad [\text{kg/s}] \quad , \quad (5)$$

where:

Δp - pressure difference between the STRING cold mass (mean value of sensors: PT1491, PT2411, PT2491, PT3411) and line D (sensor PT9446) [bar],

ρ - helium density in the cryostat [kg/m^3],

k_v - coefficient of the quench relief valve,

$\sqrt{998.5} / 3600$ - coefficient converting [m^3/h] into [kg/s].

Helium flow out of the string calculated for run 633 is shown in figure 10. An integrated flow is equal to 119.94 kg. The number corresponds well with an average of 120 kg of helium expelled from the string after a quench. Enthalpy flow is

$$h_{flow} = \dot{M} h_{He} \quad [\text{J/s}] \quad . \quad (6)$$

Enthalpy flow for run 633 is shown in figure 11. For other runs one gets slightly different numeric values, but the time evolution of the helium characteristics is similar.

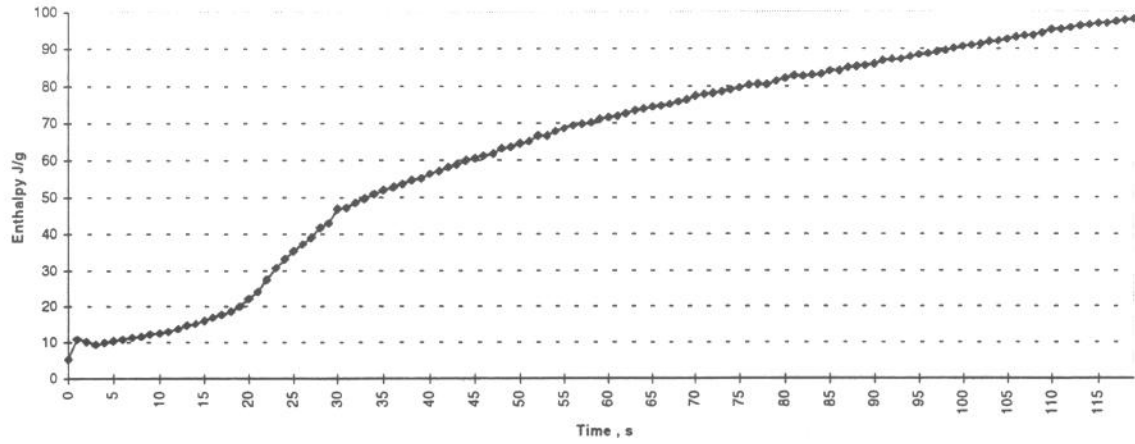


Fig.9. Enthalpy of helium leaving the string cold mass, run 633.

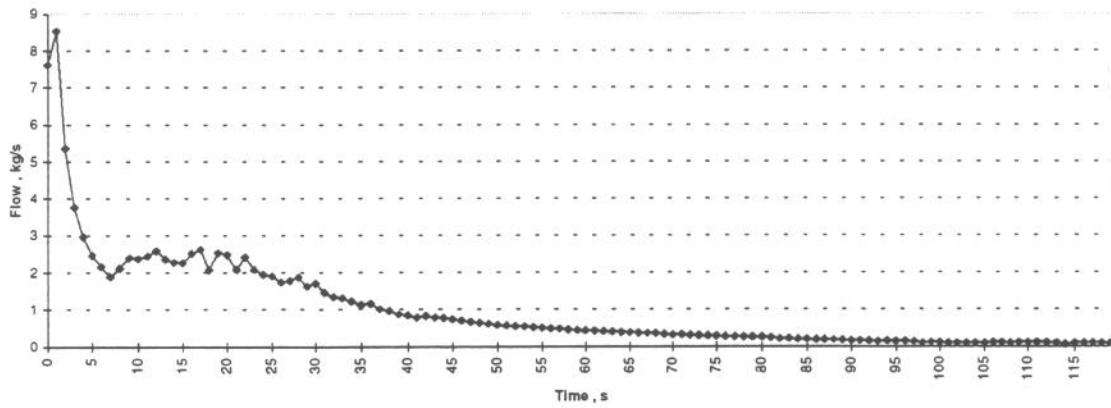


Fig.10. Helium mass flow out of the string cold mass, run 633, quench valve $k_v = 33$.

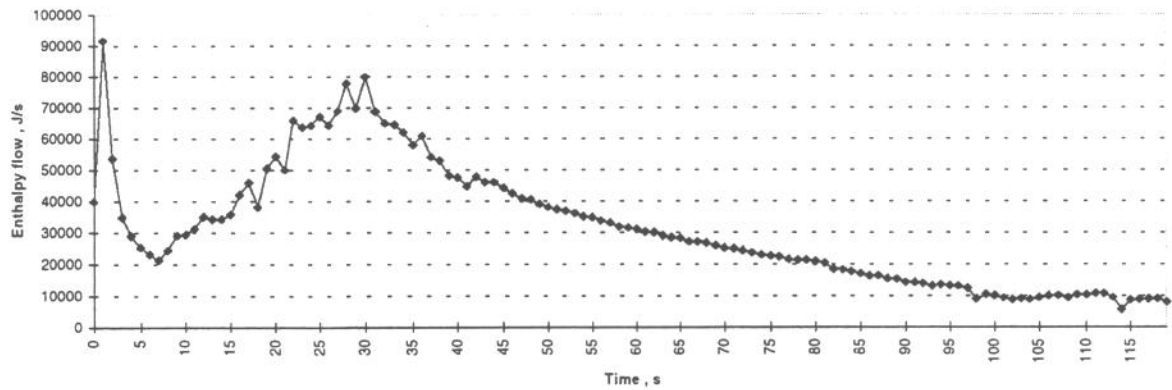


Fig.11. Enthalpy flow out of the string cold mass, run 633.

Figure 12 shows the dependence of the enthalpy calculation on the choice of sensors measuring parameters inside the string cold mass (for run 633). If the temperature and pressure are taken as mean values of sensors located in vicinity of dipole 2, one gets the results best matching the string heat balance calculation. In this case average helium enthalpy is equal to 31.68 J/g . The number lies within the statistical error of enthalpy estimation (mean value plus/minus its standard deviation) - see table 2.

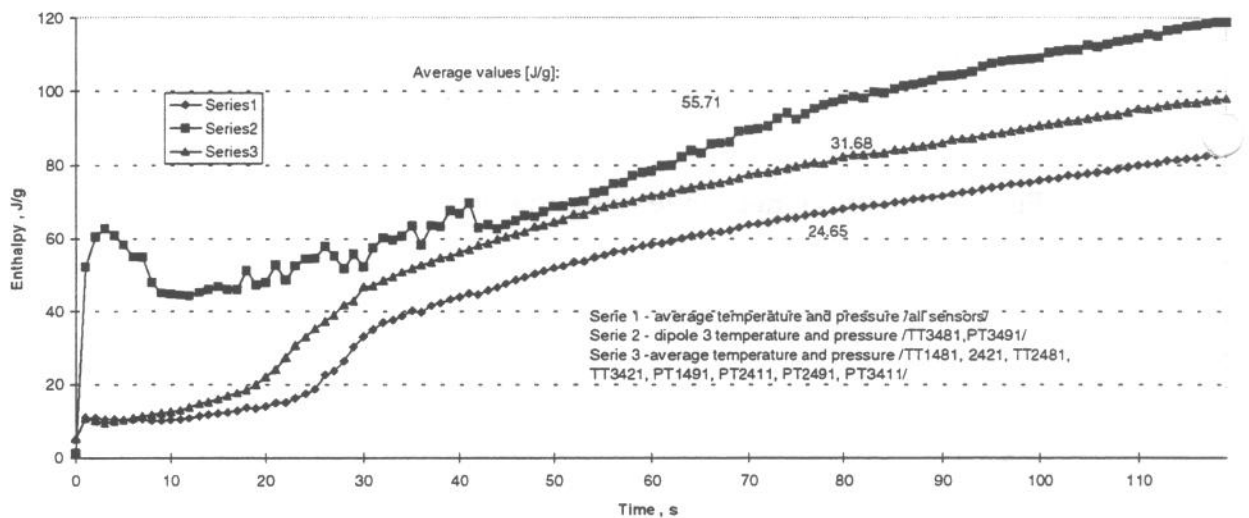


Fig.12. Enthalpy of helium leaving the string cold mass, run 633.

4.3. Best estimation of the enthalpy of helium leaving the cold mass.

As it was already mentioned the enthalpy of helium leaving the cold mass is basic input for any further consideration. An average helium enthalpy has been calculated of the string energy balance and of enthalpy flow leaving the cold mass - table 2.

Table 2. Average helium enthalpy.

Method of calculation	String energy balance /runs 613,626,633,635,638,651, 653 675,677,692,842 , statistical analysis/.	Enthalpy flow /run 633/
Average enthalpy , J/g	33.29	31.68
Standard deviation , J/g	2.36	-
Range of change , J/g	30.93 - 35.65	-

On the following we shall use a value of 33.29 J/g. The higher enthalpy value will be used as the input data to foresee the highest possible pressure and temperature in line D.

5. Simulations of helium parameters in line D after a quench.

Line D is one of the nodes of the helium recovery system. If we assume that the line is an adiabatic wall without heat capacity and neglect potential and kinetic energy of incoming helium, then equation (1) takes the form

$$dU = h_{He} dM_{He\text{-expelled}} \quad (7)$$

The increase of energy caused by the quench of one half-cell is

$$\Delta U = \bar{h}_{He} \Delta M \quad (8)$$

where: ΔU - energy change,

\bar{h}_{He} - average enthalpy of helium leaving the half-cell,

ΔM - mass of helium leaving the half-cell.

5.1. Equilibrium parameters in line D, as a function of number of half-cells quenched.

The helium parameters in the line D stabilize several minutes after a quench. Then the temperature and pressure can be calculated as a function only of the number of half-cells quenched, taking the enthalpy of the discharged helium as a parameter - see figures 13 and 14.

Initial conditions:

Temperature in line D - 20 K (nominal temperature in line D)

Pressure in line D - 130 kPa (nominal pressure in line D)

Length of line D - 3400 m, volume of line D - 60.08 m³ (for one LHC sector)

Average enthalpy of helium entering line D - 33.29 J/g

Average mass of helium leaving one half-cell - 120 kg

As follows from figure 14, the capacity of line D is high enough to accumulate the helium discharged from the magnets cold mass, if the number of half-cells quenched does not exceed 44. The simulation results can be shown on a temperature-entropy diagram - figure 15. As follows from the diagram the final parameters of helium in line D are far away from the two-phase region. They would enter the two phase region only if the average enthalpy of the discharged helium were lower than 18.55 J/g.

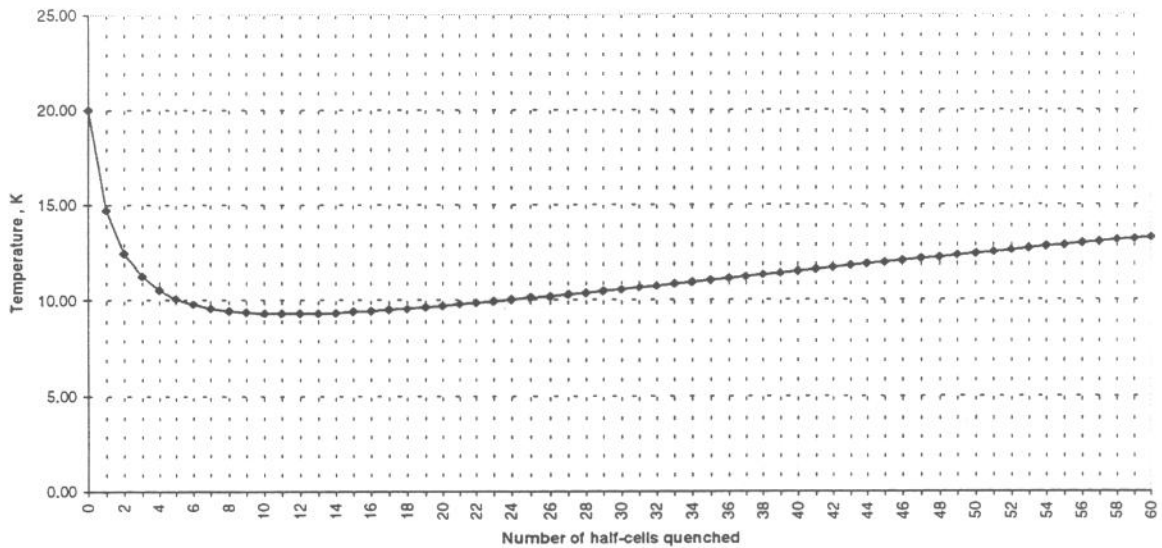


Fig.13. Temperature in line D as a function of the number of half-cells quenched, enthalpy of the discharged helium 33.29 J/g.

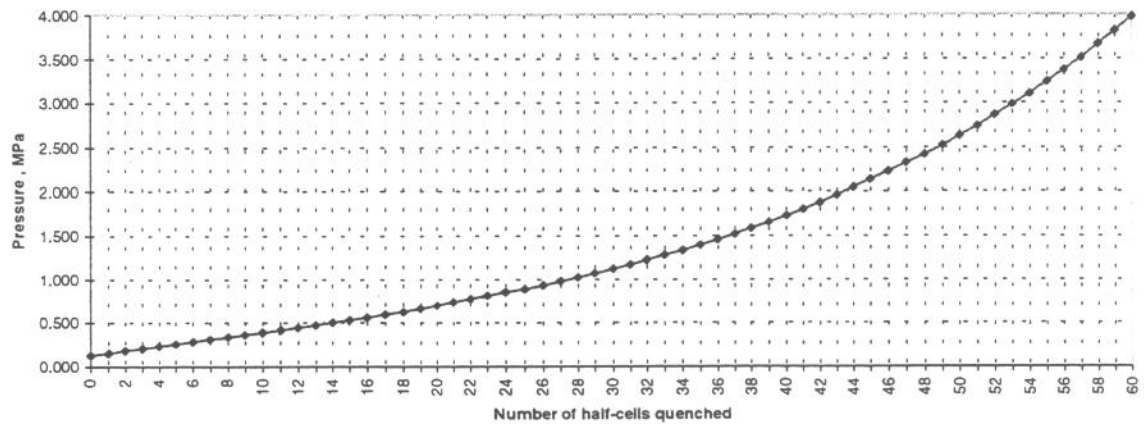


Fig.14. Pressure in line D as a function of the number of half-cells quenched, enthalpy of the discharged helium 33.29 J/g.

5.1.1. Influence of the heat capacity of line D.

The heat capacity of line D does not influence the simulation results in a significant way and it is then negligible - see figure 16.

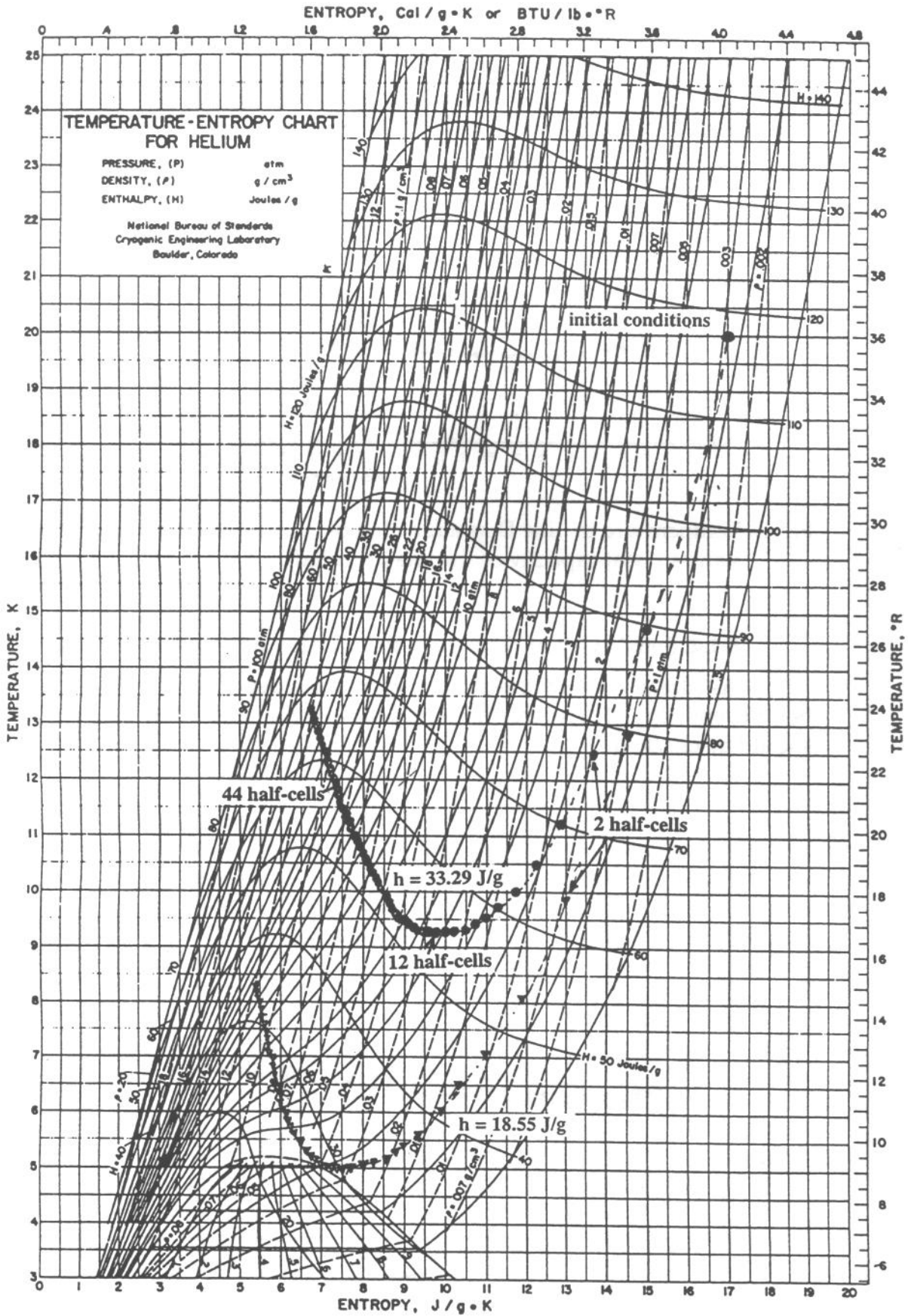


Fig.15. Evolution of final parameters in line D with increasing number of half-cells quenched.

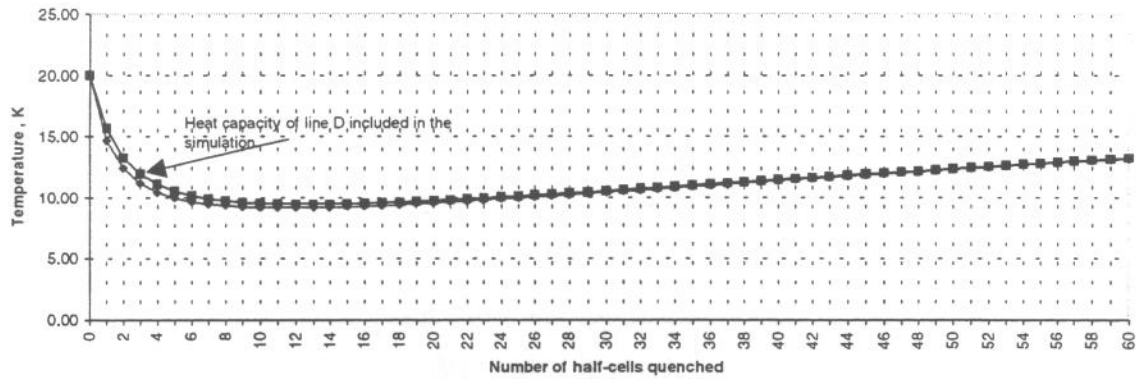


Fig.16. Temperature in line D as a function of number of half-cells quenched, upper values - heat capacity of the line included.

5.1.2. Sensitivity of the results to enthalpy of the discharged helium.

As already stated the simulation results dependent strongly on the value of helium enthalpy. Therefore the sensitivity of the simulation results to the enthalpy should be checked.

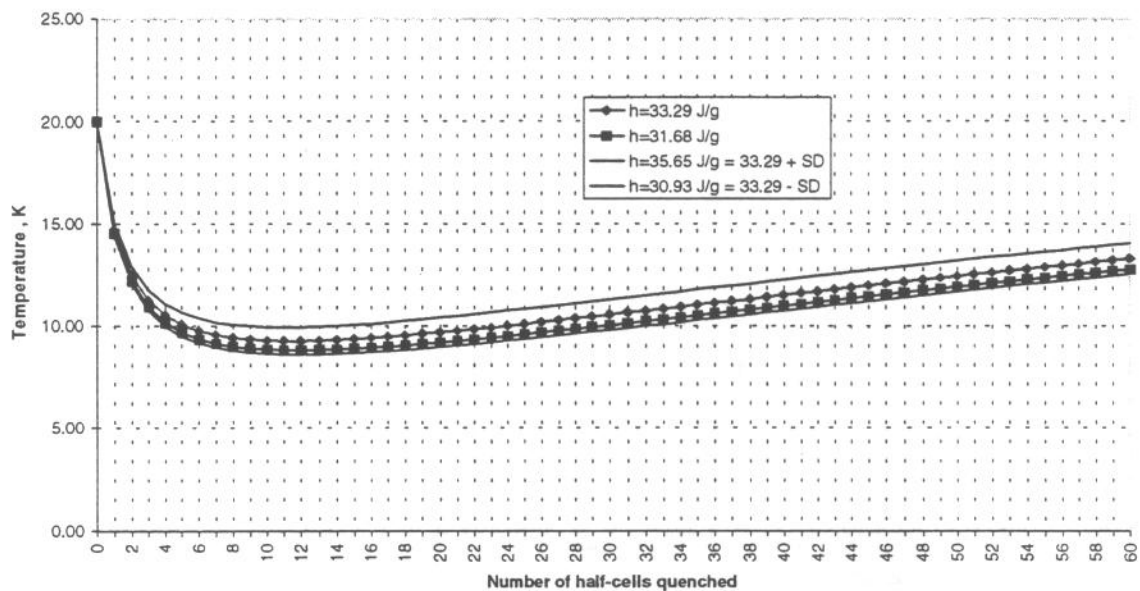


Fig. 17. Influence of enthalpy of the discharged helium on the final temperature in line D.

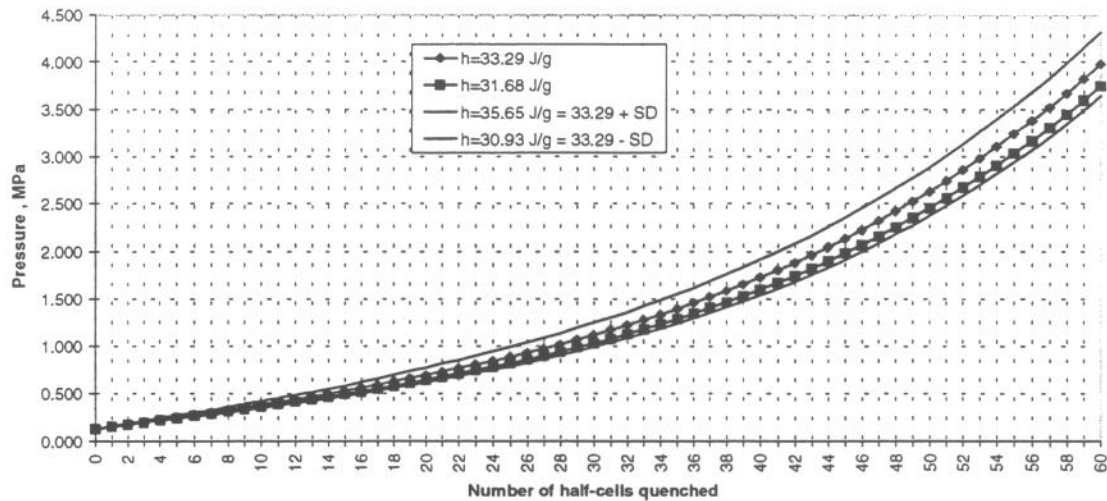


Fig.18. Influence of enthalpy of the discharged helium on the final pressure in line D.

The enthalpy of the discharged helium was varied between 30.93 and 35.65 J/g i.e. its mean value plus and minus the standard deviation - see table 2. Within the enthalpy change the final temperatures in line D may differ by 1.5 K (fig.17) and pressures by 0.1 MPa for a 14 half-cells quench and by 0.4 MPa for 42 half-cells quench (fig.18). It means that in case of a sector quench line D may only be capable of recovering helium expelled from 41 half-cells instead of 44.

5.2. Dynamic characteristics of line D as a closed volume (no outflows).

With a known value of helium enthalpy and mass flow (figures 9 and 10) one can calculate the temperature and pressure in line D during a discharge from cold mass. Equation (7) takes the form

$$dU = h_{He}(t)\dot{m}(t)dt \quad , \quad (9)$$

where $h_{He}(t)$ and $\dot{m}(t)$ - enthalpy and mass flow of helium, t - time.

Line D is treated as a lumped-parameter node with one flow input. The basic assumption is that the equilibrium energy balance equation (9) can be used during a discharge. The dynamic characteristics will be shown for a "small" quench (2 half-cells), "medium quench" (28 half-cells) and whole sector quench (54 half-cells). Enthalpy flow out of one half-cell is shown in figure 11. The average enthalpy is equal to 31.68 J/g and the integrated helium mass flow is equal to 119.8 kg.

"Small" quench - 2 half-cells.

Time evolution of temperature and pressure in line D after a quench of two half-cells are shown in figures 19 and 20. In case of a "small" quench no liquid is present in line D, even for a short period of time.

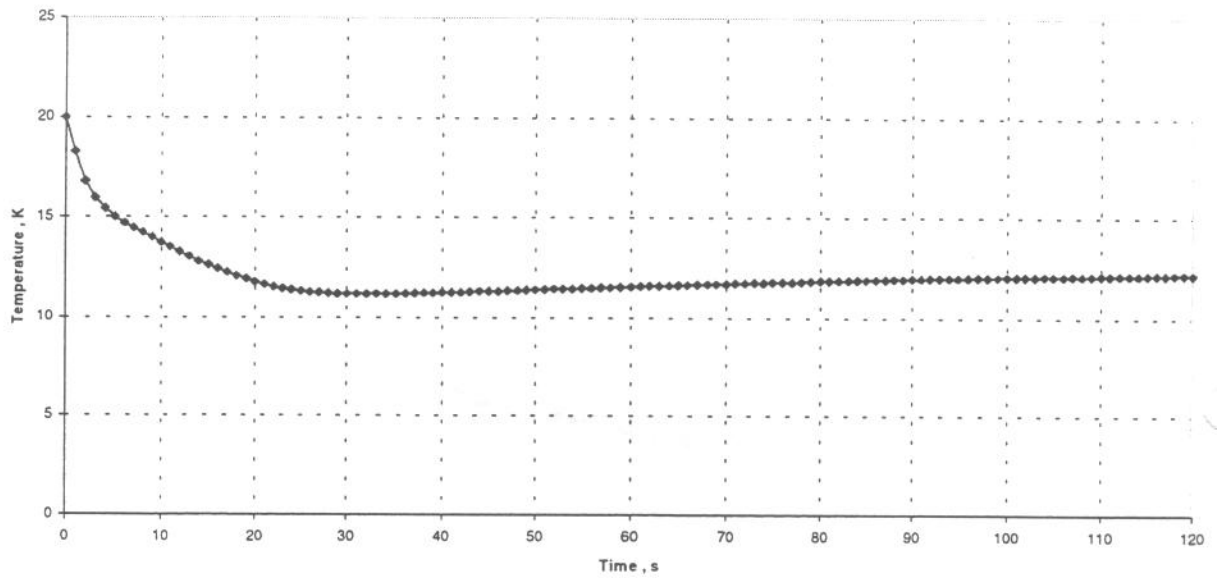


Fig.19. Temperature in the line D after a quench of 2 half-cells. Data based on run 633.

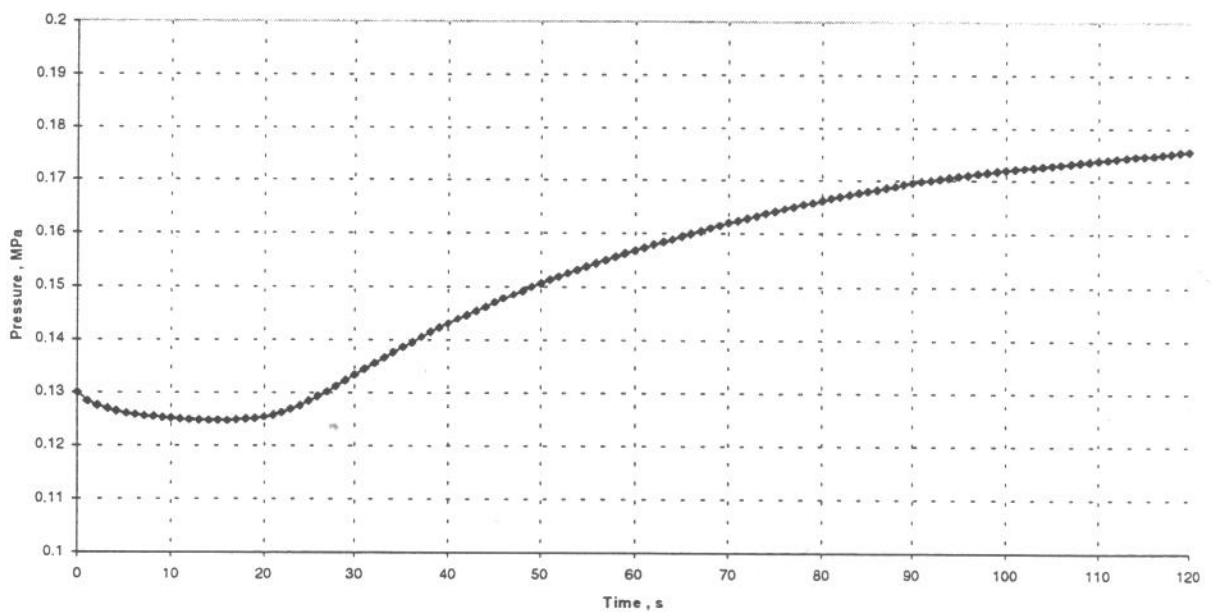


Fig.20. Pressure in the line D after a quench of 2 half-cells. Data based on run 633.

“Medium” quench.

If the number of half-cells quenched exceeds 12, then liquid helium can be observed in line D for some time. Figures 21 to 23 show temperature, pressure and vapour quality in line D after a quench of 28 half-cells.

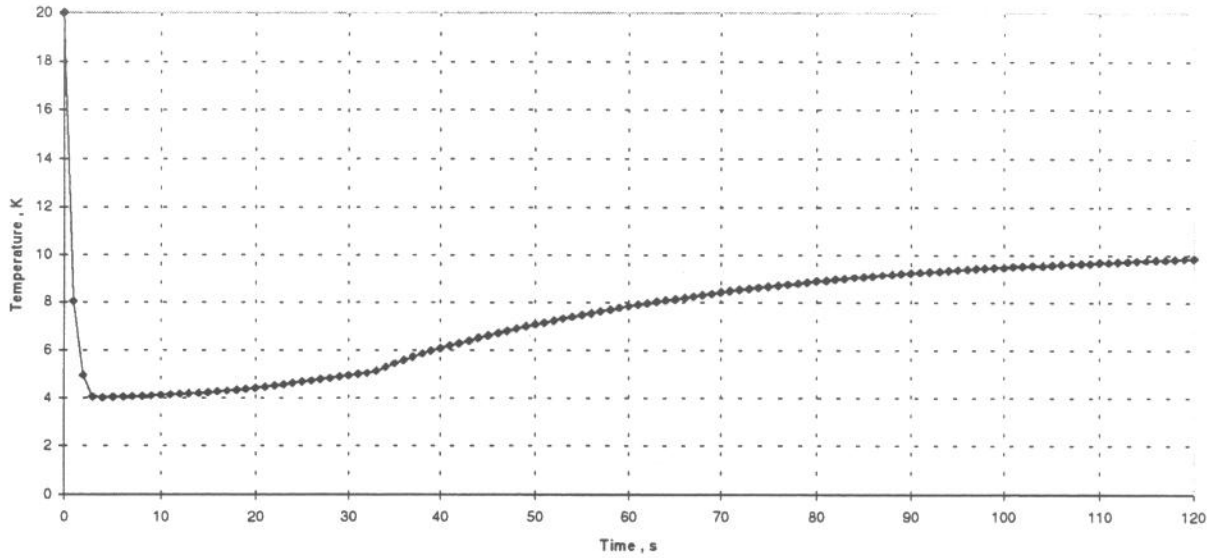


Fig.21. Temperature in line D after a quench of 28 half-cells. Data based on run 633.

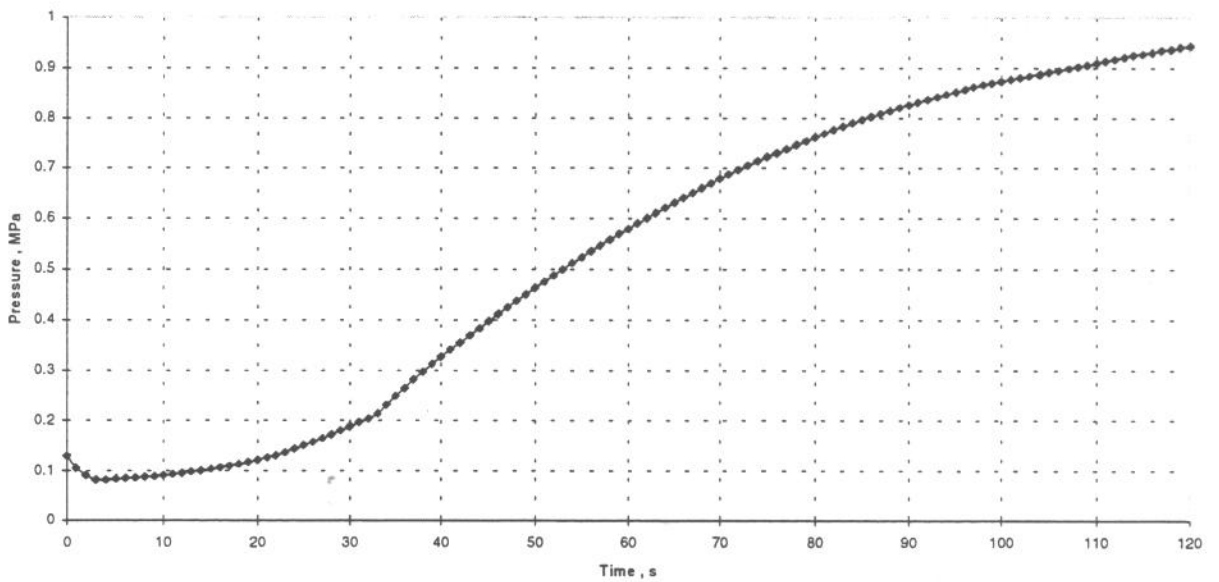


Fig.22. Pressure in line D after a quench of 28 half-cells. Data based on run 633.

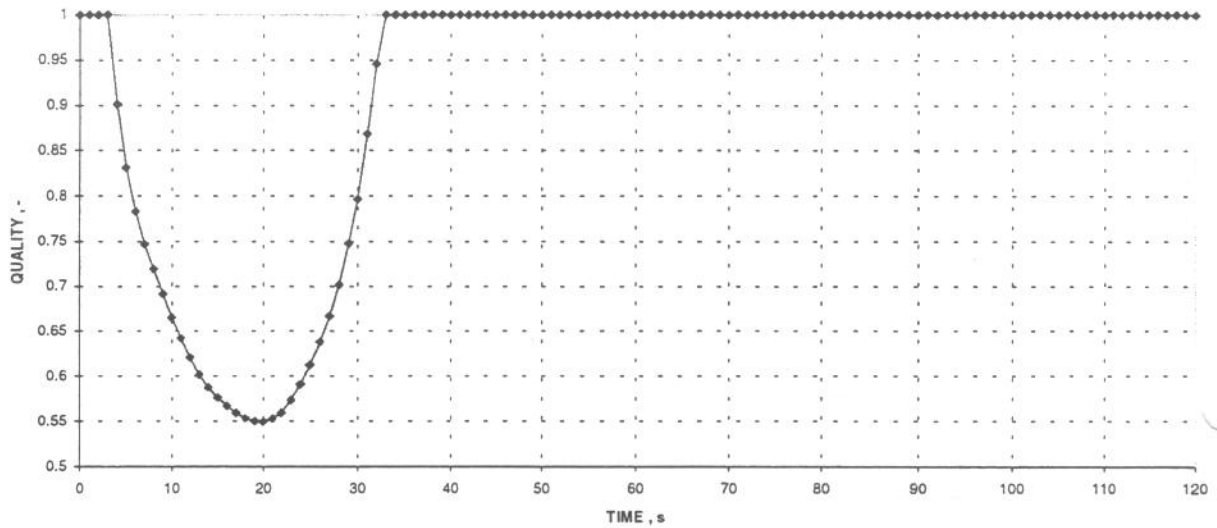


Fig.23. Vapour quality in line D after a quench of 28 half-cells. Data based on run 633.

Whole sector quench.

Finally, for a total sector quench (54 half-cells) one gets the results shown in figures 24 to 26.

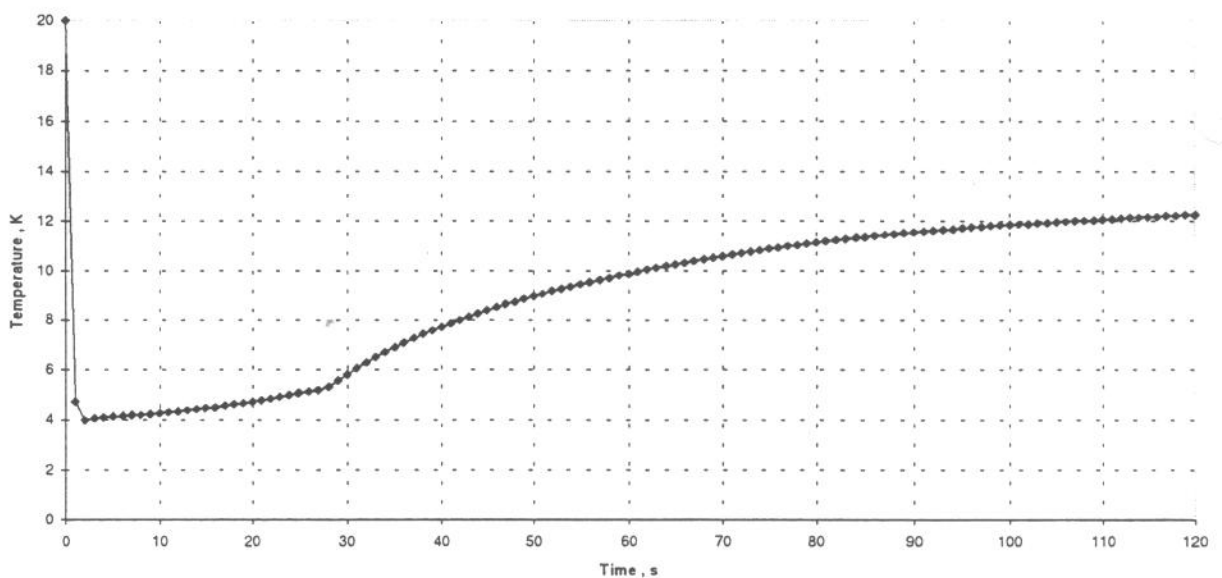


Fig.24. Temperature in line D after a quench of 54 half-cells. Data based on run 633.

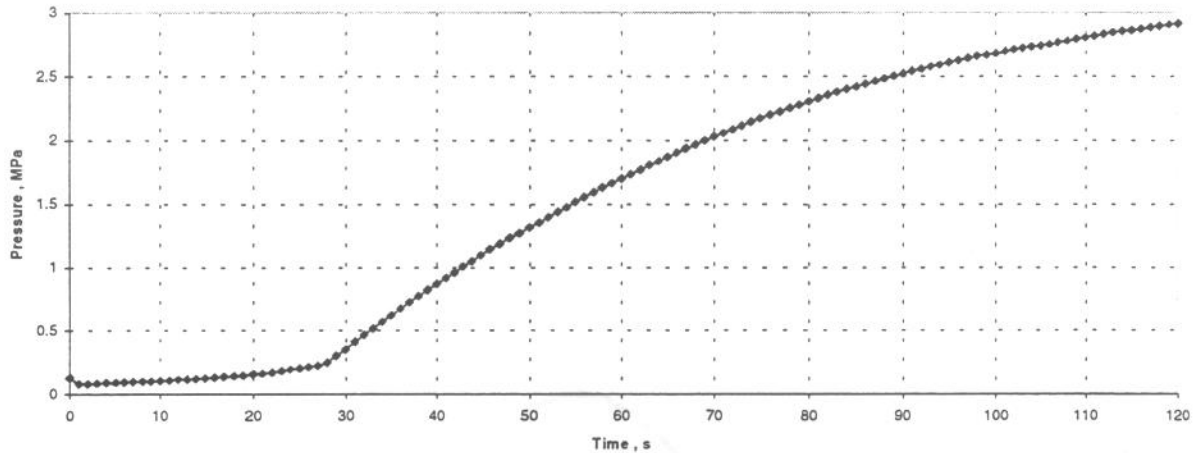


Fig.25. Pressure in line D after a quench of 54 half-cells. Data based on run 633.

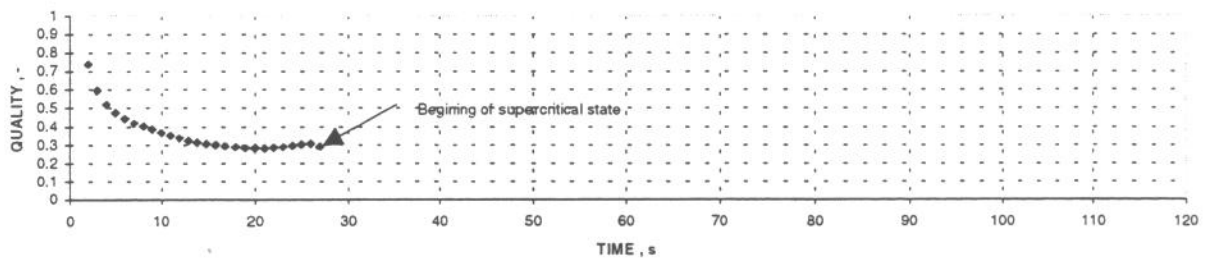


Fig.26. Vapour quality in line D after a quench of 54 half-cells. Data based on run 633.

Line D forms a buffer which can accumulate expelled helium if the number of quenched half-cells does not exceed 44. For a higher number of half-cells pressure inside line D increases over 2 MPa i.e. its design pressure. It means that in case of a whole sector quench some helium must be discharged from line D.

5.3. LHC quench classification.

According to the number of half-cells involved, LHC quenches can be classified from their cryogenic consequences as:

- “small” quench (2-12 half-cells quenched), no liquid present in line D during discharging, maximal pressure in line D equal to 0.42 MPa after a quench of 12 half-cells, small quench can be fully buffered by the capacity of line D,
- “medium” quench (13-44 half-cells quenched), liquid helium present for some time in the line D, maximal pressure 2 MPa (for 44 half-cells), can be buffered by the capacity of line D for a short time,
- large- whole sector- quench (45-54 half-cells quenched), can not be fully buffered by line D.

5.4. Dynamic characteristics of line D with an outflow.

If the number of quenched half-cells exceeds 44, the pressure in line D will increase above 2 MPa. To maintain the pressure below that limit it is necessary to let some helium out of the line. In this case line D becomes a node with one flow in and one flow out. Assume the helium outflow to be discharged through a valve opening on pressure. Let the valve open, if the pressure in line D exceeds 1 MPa. Then the outflow (figure 27) may be calculated according to the formula (5), where: Δp - pressure difference in line D and 1 MPa (for pressures equal or lower than 1 MPa, the outflow is equal to zero), r - helium density in line D, $k_v = 70$.

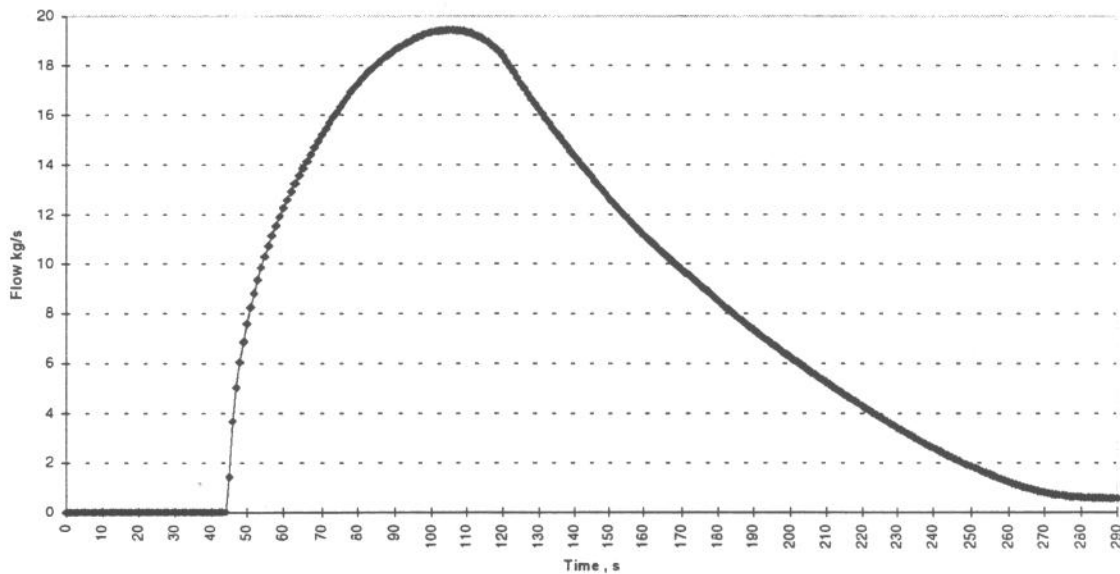


Fig.27. Outflow from line D through a valve opening on pressure at 1 MPa, $k_v = 70$.

In case of a whole sector quench the helium flow out of line D may be as high as 20 kg/s. Such a high flow exceeds the capacity of the LHC refrigerators. It means that a fraction of the helium would have to be either warmed up and accumulated in medium pressure storage tanks or relieved to the environment.

The dynamic behaviour of line D connected with a medium pressure storage vessel was investigated by L. Brue [5]. The approach was based on a one dimensional dynamic model. As follows of [5] the pressure oscillations in line D are not significant and do not exceed 0.3 bar and 0.7 bar in case of quenches of five half-cells and a whole sector, respectively.

Steady state pressures given in L. Brue's work are lower than those presented in this note because of two reasons:

1. Input helium enthalpy value assumed by L.Brue was relatively low - about 20 J/g (prototype magnet string results were not available then).
2. Line D was modelled as one volume together with the medium pressure gas reservoir.

Figures 28 to 30 show time characteristics of line D after a quench of 54 half-cells with the outflow shown in figure 27.

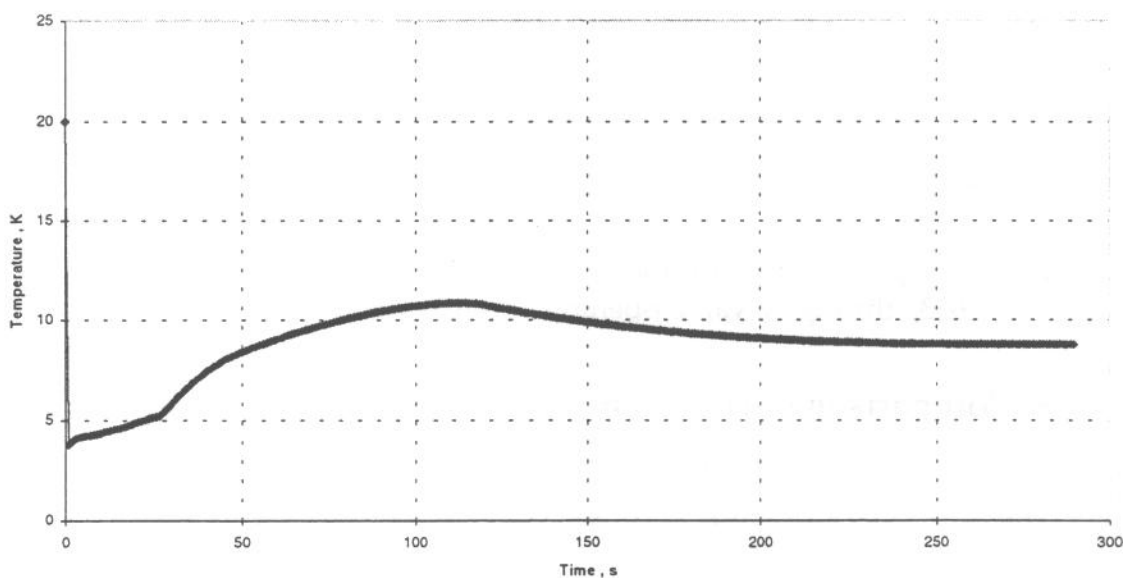


Fig.28. Temperature in line D after a quench of 54 half-cells. "Flow in" based on run 633. "Flow out" through a valve opening on pressure at 1 MPa, $k_v = 70$.

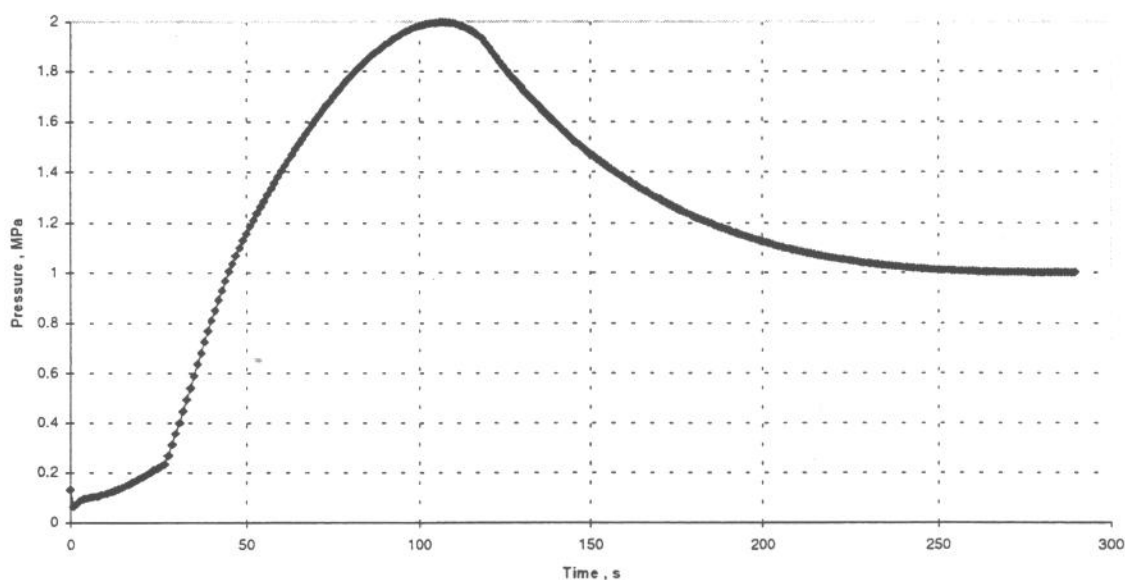


Fig.29. Pressure in line D after a quench of 54 half-cells. "Flow in" based on run 633. "Flow out" through a valve opening on pressure at 1 MPa, $k_v = 70$.

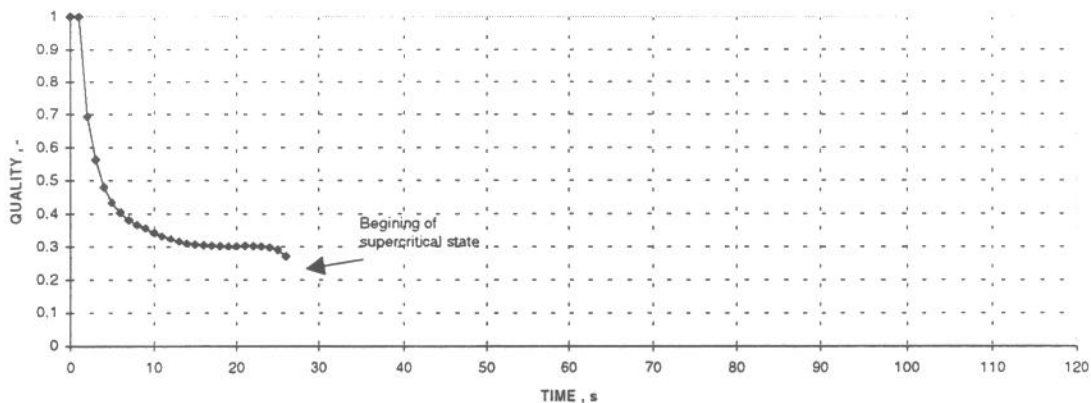


Fig.30. Vapour quality in line D after a quench of 54 half-cells. Outflow based on run 633, through a valve opening on pressure at 1MPa, $k_v = 70$.

6. Comparison of simulation results with the string experimental data.

6.1.The string as a model of the LHC recovery system.

The prototype string line D consists of two parts (see figure 2):

- pipe D , volume 0.88 m^3
- quench buffers vessel (QBV), volume 2 m^3

The total volume of string line D is then 2.88 m^3 .

The total volume of LHC line D is 60 m^3 .

From the point of view of helium recovery system and assuming equilibrium distribution of helium, the string quench is then a model of a 21 half-cells LHC quench.

As follows from figure 14 the final pressure in the string buffer vessel without an outflow should not exceed 0.75 MPa. The number corresponds well to the pressure observed during the string first quench performed without an outflow to a balloon, and a safety valve set at 0.8 MPa [6].

6.2.Simulation of string quench, comparison with experimental data.

In a present configuration the string buffer vessel is equipped with valves which let a portion of helium out of the system after a quench:

- Pressure actuated valve PV9451 opening when the pressure in the quench buffer vessel QBV exceeds 2.1 bar, the valve connects the buffer vessel with the balloon. To protect a balloon against too rapid input flow, the valve closes when the pressure reaches 2.2 bar.
- Pressure safety valve PSV9453 opening when the pressure in the vessel exceeds 4.5 bars.

From balloon filling measurements, it can be seen that a small amount of helium (about 5 m³ in normal conditions) leaves the buffer vessel in the pressure range 2.1-2.2 bars. Then the buffer vessel remains closed until the pressure reaches 4.5 bar and the safety valve PSV9453 opens. Finally about 200 m³ of helium (in normal conditions) leave the buffer vessel.

Helium parameters in string line D have been simulated for the outflow corresponding to the above remarks, enthalpy and helium flows were based on run 633.

The comparison of measured (run 633) and simulated temperature in the quench buffer vessel is shown in figure 31.

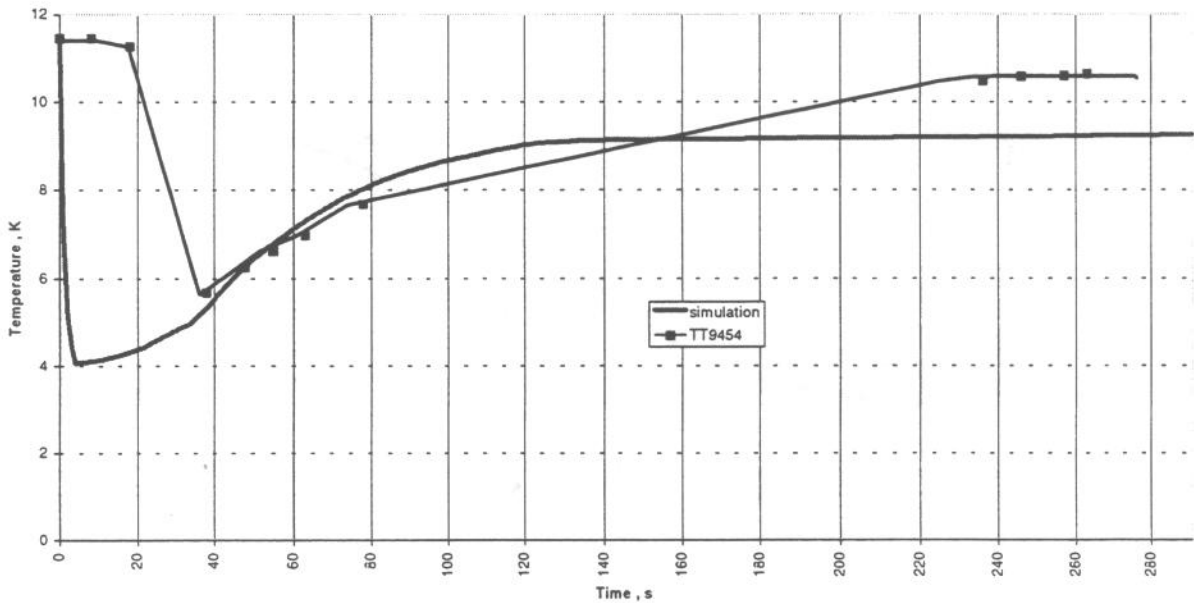


Fig. 31. Temperature in the string quench buffer vessel. Comparison of simulation results and experimental values -run 633. Initial temperature - 11.45 K.

The measured temperatures are delayed by about 20 s in comparison with the simulation results. This is caused by the fact that pipe D connecting the String with the buffer vessel introduces a transport delay to the buffer vessel dynamics, which is not taken into account in the simulation. The measured temperature is slightly higher (up to 1.5 K) than that simulated. This results from buffer vessel heat capacity and heat inleaks which were neglected in calculations.

Figure 32 shows the calculated and measured pressure in the buffer vessel. Similar like in case of temperature, the experimental results are affected by pipe D transport delay.

One of the useful parameters for comparing the experimental and simulation results is the vapour quality in the quench buffer vessel. The measurement of the

liquid level (sensor LT9452) in the buffer vessel is affected by a high level of noise, hence the comparison has a rather qualitative character. It can be seen from figure 33, that according to the simulation, the liquid should be present in the buffer vessel in the time period between 5 and 35 seconds after the quench, while it is experimentally detected by sensor LT9452 between 22 and 45 seconds. The time delay corresponds well to that observed for temperature and pressure - see figures 31 and 32. When the pressure in the buffer vessel exceeds the critical value, no liquid is detected.

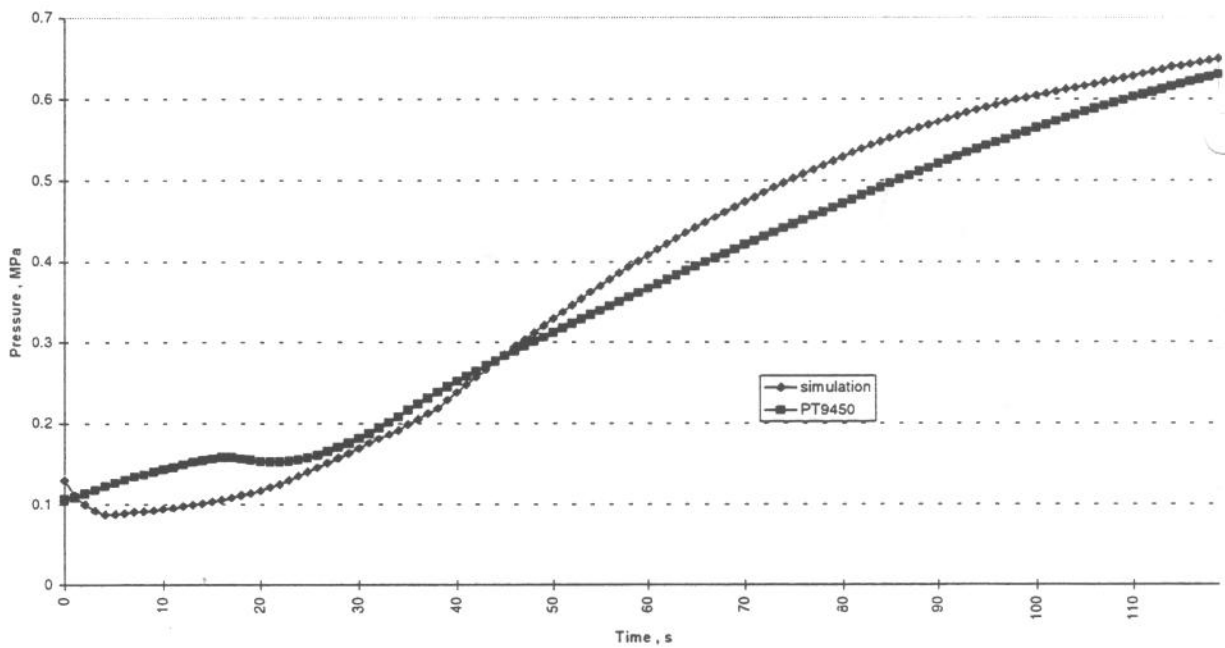


Fig. 32. Pressure in string buffer vessel. Comparison of simulation results and experimental values - run 633, pressure sensor PT9450.

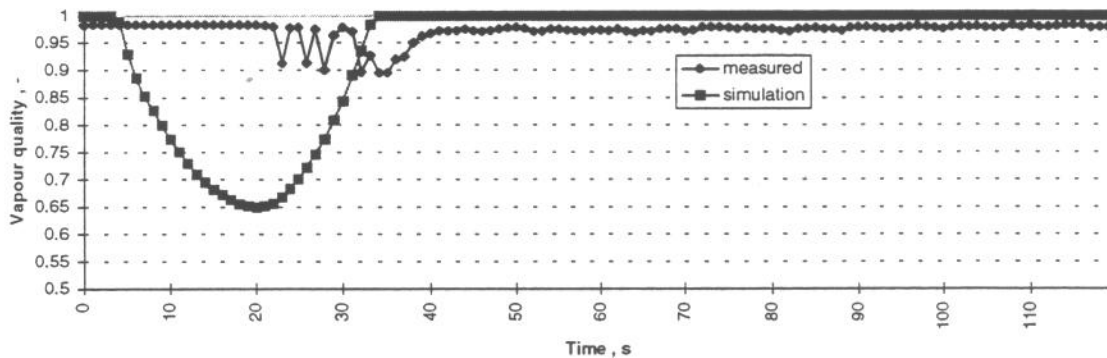


Fig. 33. Vapour quality in the STRING buffer vessel. Comparison of simulation results and experimental values - run 633, liquid helium level sensor LT9452.

As follows from figures 31 to 33, a lumped parameter approach produces results in good agreement with the string experimental data. Hence this method will be used for simulating other elements of the helium recovery system.

7. Simulation of helium recovery in medium-pressure (MP) gas tanks.

Medium-pressure (2 MPa) gas storage will be installed for operational flexibility, enabling in particular the immediate recovery of the helium discharged from line D after a quench [7] - see figure 1. The foreseen total volume is either 1000 m³ or 1500 m³ per sector. As 500 m³ is foreseen to enable a smooth operation of a sector refrigerator, a volume of 1000 m³ will be considered as a quench buffer for each sector. On the other hand a simultaneous quench of the two adjacent sectors is quite unprobable, so it should be possible to buffer a sector quench with a medium-pressure gas tanks of a total volume 2000 m³.

As follows from the simulation of the helium parameters in line D following a quench, only in case of a whole sector quench is the capacity of line D too small to contain (even for a short time) all the helium expelled from the cold mass. The amount of helium that should be discharged from line D depends on the scenario of operation of the valve between line D and the vertical line to the MP gas tanks (see fig.1). An example of helium outflow is shown in figure 27.

As the gas tanks are made of carbon steel, the temperature of the wall must not decrease below -40 °C, so that the in-flowing helium stream should be warmed up.

There are two natural heat sources which can be used for that purpose:

1. Convective heating on the vertical uninsulated line connecting line D with the MP gas tanks.
2. Heat capacity of the MP gas tanks.

7.1. Convective heating on the vertical uninsulated line connecting line D with the MP tanks.

The LHC line D is connected with the storage reservoirs through vertical uninsulated lines the lengths of which depend on the access point and vary from 45 to 145 m. The lines exchange heat with the environment in a natural convection process and with the helium flowing inside them, in a forced convection process.

Forced convection heat transfer from helium flowing inside the vertical line to the line.

A rough estimation of Nusselt number based on the helium flow given in figure 27 is 8000 which yields a heat-transfer coefficient of $a = 1900 \text{ W/m}^2\text{K}$.

Free convection heat transfer from the environment (air, 290 K, 1 bar) to the line.

An amount of heat that can be transferred to helium flowing through a vertical line is limited by the free convection heat transfer from the environment to the line.

The heat transfer to a vertical line connecting line D with a medium-pressure gas storage vessel is a free convection process and it can be described by the equation (11)

$$Nu = C(Gr Pr)^n \quad (11)$$

Nu - Nusselt number, Gr - Grashof number, Pr - Prandtl number, C and n - coefficients depending on the GR*Pr value.

Although heat transfer to the vertical line is not a steady process, the Nu, Gr, and Pr numbers can be estimated for the following conditions:
 temperature in the shaft - 290 [K] (temperature of the warm undisturbed air),
 air pressure in the shaft - 100 [kPa],
 vertical line wall temperature - 50 [K],

Air parameters calculated for 170 K (the mean temperature of the pipe wall and warm undisturbed air) and 100 Pa are:

conductivity $\lambda = 0.01590$ [W/mK],

density $\rho = 2.0555$ [kg/m³],

heat capacity $c_p = 1015.33$ [J/kgK],

dynamic viscosity $\eta = 11.53 \cdot 10^{-6}$ [Pa s],

kinematic viscosity $\nu = 5.609 \cdot 10^{-6}$ [m²/s],

coefficient of volume expansion $\beta = 0.5962 \cdot 10^{-2}$ [1/K],

Prandtl number $Pr = 0.7351$ [-],

temperature difference between a wall and undisturbed air (estimation) $\Delta T = 150$ K.

The Grashof number is equal to:

$$Gr = gd^3\beta\Delta T / \nu^2 = 2.230 \cdot 10^9 \quad (12)$$

For $Gr \cdot Pr = 2.230 \cdot 10^9 \cdot 0.7351 = 1.64 \cdot 10^9$ the coefficients in Eq. (11) are equal: $C = 0.135$ and $n = 0.333$, then $Nu = 160$ and a convection heat transfer coefficient α is equal to

$$\alpha = \frac{Nu \cdot \lambda}{d} = 12.7 \text{ [W/m}^2\text{K]} \quad (13)$$

If we assume a 50% efficiency of a heat exchange process (e.g. due to the ice covering the line) and a 50 K average temperature difference between a pipe wall and undisturbed air, we get a following heating power for a vertical line in different access points - table 3.

As it appears on table 3, the free convection heating power is equal to 0.4 kW per meter of a vertical line, which is not sufficient to warm helium entering the medium-pressure gas storage tanks.

Table 3. Free convection heating power of vertical lines and pressure drops at the different access points.

Point number	Shaft depth - length of vertical line, m	Pressure drop kPa	Free convection heating power of vertical line, kW
P2	42	42	17
P4	145	145	58
P6	86	86	34
P8	82	82	33

Pressure drop in the vertical line.

Pressure drop can be calculated by the following formula:

$$\Delta p = \lambda \frac{\rho v^2}{2} \frac{l}{d} \quad (14)$$

where: λ - pressure drop coefficient, ρ - helium density inside the vertical pipe, v - fluid velocity, l, d - pipe length and diameter.

Roughly estimated, helium parameters in a vertical line are:

pressure - 1 MPa, temperature - 50 K, Pr - 0.7167,
dynamic viscosity - $0.6531 \cdot 10^{-5}$, helium mass flow - 10 kg/s

For the 0.2 m tube diameter, the Reynolds number is $Re = 10^7$, and the pressure drop coefficient is given by:

$$\lambda = 0.032 + 0.221/Re^{0.237} = 0.0368 \quad (15)$$

A pressure drop for a 1 m length is 1 kPa. Estimated pressure drops for vertical lines at the different points are given in table 3.

7.2 Heat capacity of the medium-pressure gas tanks.

The medium-pressure gas tanks are composed of a number of cylindrical pressure vessels of horizontal axis characterised by the following technical parameters:

Wall material - carbon steel,
density 7850 kg/m^3 , heat capacity 450 J/(kgK) .
Dimensions - length 28.2 m, diameter 3.5 m, volume 250 m^3 .
Mass - 56400 kg.
Wall surface area - 330 m^2 .

It is assumed that a whole sector quench will be buffered with 8 (4 at each end of the sector) medium-pressure tanks of a total volume 2000 m^3 . In the lumped parameter approach eight tanks form a mass of 451.2 ton with a heat exchange surface 2640 m^2 and an integrated heat capacity 25.38 MJ/K .

7.3 Helium parameters in MP tanks during discharge of line D.

Helium parameters in the medium-pressure gas tanks are calculated for the following assumptions:

1. Initial helium temperature in the tanks - 253 K (a minimal reasonable ambient temperature).
2. Initial helium pressure in the tanks - 100 kPa.
3. Helium flow - like outflow from line D shown in figure 27, integrated flow - 2340 kg.
4. Helium enthalpy - calculated for pressures and temperatures in line D during discharge (figures 28 and 29).
5. Convection heating power on the vertical uninsulated line - 17 kW (as for point P2, tab. 3).
6. Ideal mixing of helium inside the tanks.
7. No temperature gradient across the tank wall.
8. Forced convection heat exchange between the tank wall and helium inside, heat transfer coefficient is estimated $58 \text{ W}/(\text{m}^2\text{K})$.
9. Natural convection heat exchange between the tank wall and ambient air, heat transfer coefficient is estimated $10 \text{ W}/(\text{m}^2\text{K})$.

Figures 34 and 35 show temperature and pressure in the medium-pressure tanks calculated for the above assumptions. The temperature of the tank wall decreases by 8 K only reaching 245 K and it lies well above its lower limit (233 K). It means that the tanks heat capacity is high enough to warm up the in-flowing helium and to prevent the tanks against forbidden temperature drop. The safety margin on temperature drop is 150%. Nevertheless it must be stressed out that the heat capacity of the tanks may be fully used only if a good mixing of helium inside the tanks is guaranteed.

Warm-up of helium leaving line D due to heat in-leaks.

Several minutes after a LHC sector quench, the conditions in line D will stabilize. The natural heat inleak to line D is approximately $0.02 \text{ W}/\text{m}$ [8]. For a whole sector, and taking a safety factor of 1.5, the estimated heat flow to line D is equal to 102 W. To maintain a pressure in the line below a maximum value helium must flow out of the line.

If the following initial conditions are assumed:

temperature in the line D - 10 K,

pressure in the line D - 2 MPa (design value),

then maintaining pressure below 2 MPa, requires a helium mass flow no less than 1 g/s to be discharged from the line. If this mass flow is to be stored in medium-pressure gas reservoirs, the helium should be first warmed up. The required heating power is approximately 1300 W. This value lies well within convective heating powers of any of the vertical lines (see table 3) and therefore does not require any special device.

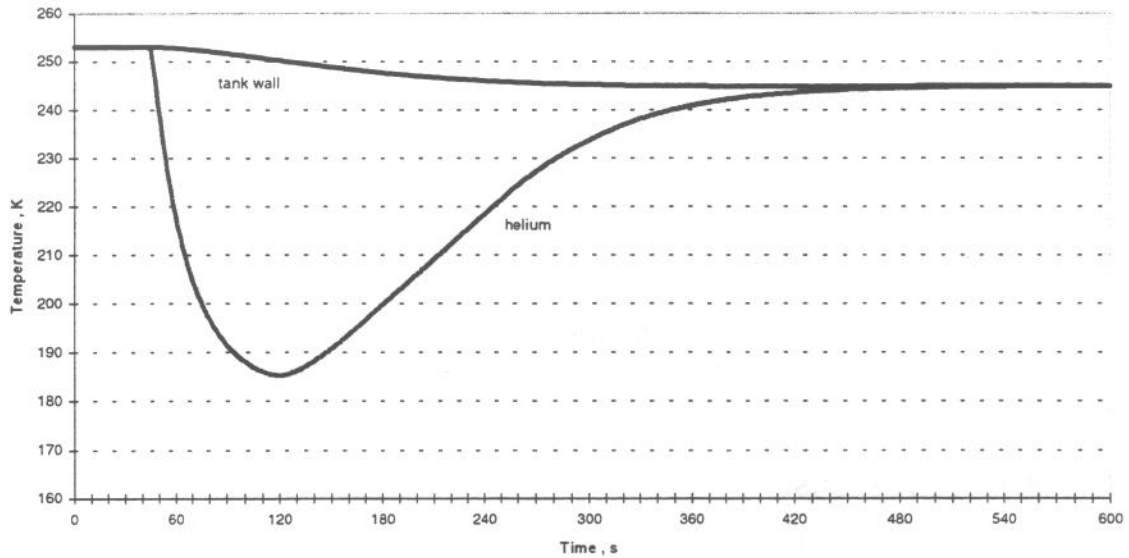


Fig.34. Wall and helium temperature in medium-pressure tanks during discharging line D, initial temperature and pressure 253 K and 1 bar respectively.

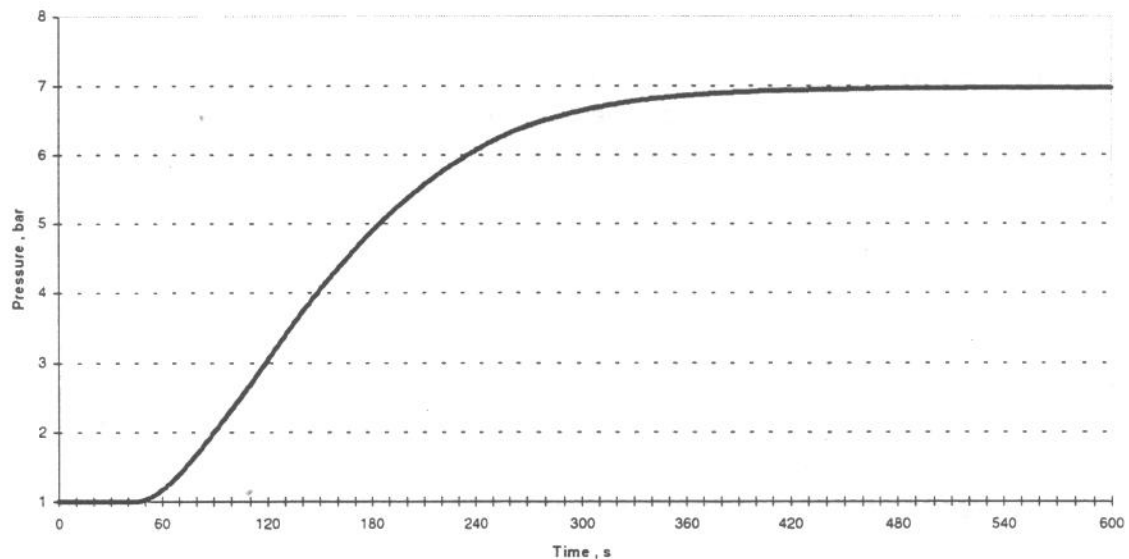


Fig.35. Pressure in medium-pressure tanks during discharging line D, initial temperature and pressure 253 K and 1 bar respectively.

8. Quench recovery.

From the LHC operation point of view, there are two most probable sizes of quenches:

- small quench - a few adjacent half-cells, considered as part of collider operation,
- whole sector quench, considered as an accidental mishap.

In case of a small quench line D can fully buffer helium expelled from the LHC cold mass. Both helium inventory and its refrigeration capacity are recovered then.

In case of a sector quench a fraction of the expelled helium (up to 30%) must leave line D and be stored in medium pressure gas tanks. As the sector refrigerator will be ready to start blowing down line D about 10 minutes after the quench, the line will store the remaining helium for that period of time. The maximum flow capacity to blow down line D to the refrigerator may vary from 780 g/s to 260 g/s [8]. If we assume that about 5000 kg of helium should be recovered from line D, it would be necessary to run the refrigerator compressors for 2 to 6 hours. It is of course necessary to provide a cryogenic load (e.g. liquefaction) for the refrigerator during the time it recovers helium vapour from line D.

After a sector quench it is then possible to recover all helium inventory and about 70% of its refrigeration (exergy).

9. Conclusions.

1. The LHC helium recovery system can be investigated with a relatively simply lumped-parameter model based on energy balance.
2. A lumped-parameter model is in good agreement with experimental data obtained on the prototype string.
3. LHC quenches can be classified from their cryogenic consequences as:
4. -"small" quench, up to 12 half-cells,
5. -"medium" quench, 12 - 44 half-cells,
6. - sector quench, 45-54 half-cells.
7. Small and medium quenches can be buffered by the capacity of line D.
8. In case of a sector quench line D is not able to accommodate all the helium expelled, and a fraction of helium (up to 30%) will have to be stored in medium-pressure gas tanks.
9. Heat capacity of the medium-pressure tanks is high enough to warm up the ir flowing helium and to prevent the tanks against temperature drop below the design value.
10. To avoid the tanks wall local temperature drop below a design limit, a good mixing of helium inside them must be achieved.
11. Convective heating along the vertical lines is efficient enough to warm up helium leaving the line D due to natural heat inleaks only.

10. References.

- [1] The LHC Study Group, The Large Hadron Collider Conceptual Design, CERN/AC/95-05(LHC).
- [2] A. Bézaguet et. al., Cryogenic Operation and Testing of the Extended LHC Prototype Magnet String, LHC Project Report 23, July 1996.
- [3] R. van Weelderen, private communication.
- [4] G. Riddone , private communication.

- [5] L. Brue, Modélisation thermohydraulique des écoulements transitoires d'hélium cryogénique induits dans la ligne de récupération du demi-octant par les transitions résistives des aimants du LHC, Note LHC 262 (1994).
- [6] L. Tavian, private communication.
- [7] L. Tavian, Stockage hélium et interconnexion des différents points du système cryogénique du LHC, Note LHC 198 (1992).
- [8] U. Wagner, private communication.
- [9] G. Krainz, private communication.
- [10] HEPAK Code by Cryodata Inc., P.O. Box 558, Niwot, CO 80544.

11. Appendixes

11.1. Appendix 1. Residual Resistance Ratio values of the outer layer coils of the string magnets [9].

	Units	LSQP	MB1	MB2	MB3
RRR A	[-]	92	113	91	84
RRR B	[-]	96	109	106	86

RRR measurement error: 3%.

11.2. Appendix 2. Helium density stratification during discharging the string through quench relief valve located close to MB3.

Figure 35 shows helium density in the vicinity of the string magnets during discharge after a 13.1 kA quench. The density stratification is confirmed by helium mass balance inside the string cold mass - see figure 36.

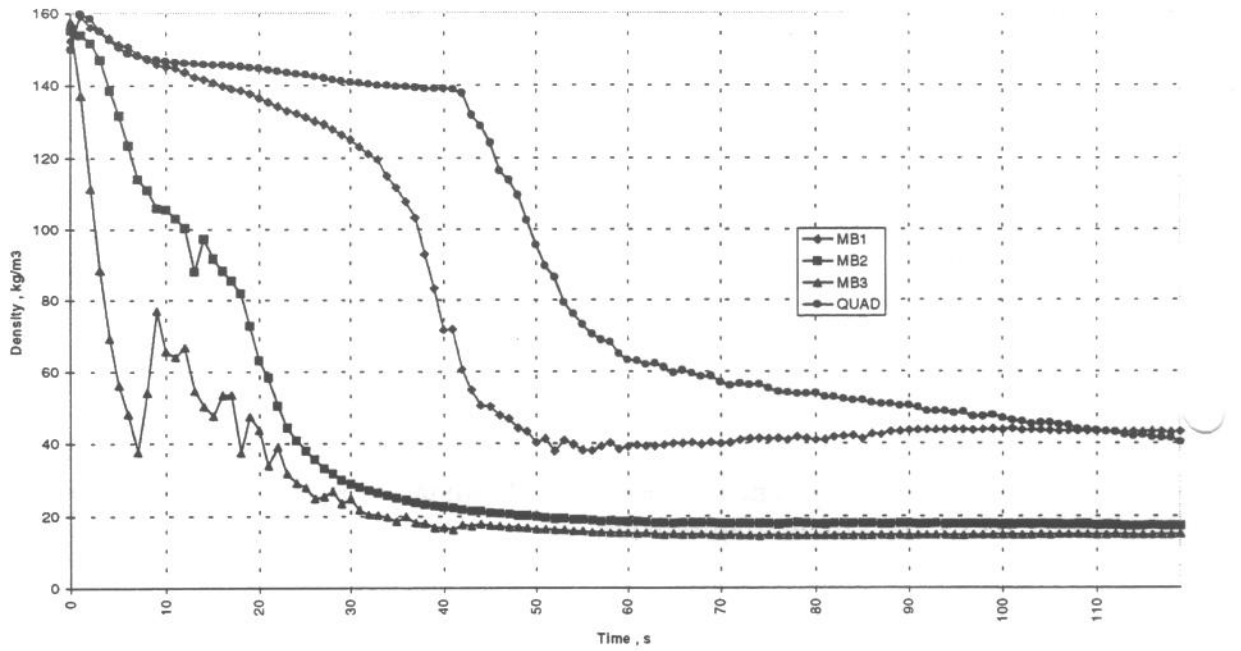


Fig.35. Helium density in the vicinity of the string magnets during discharge, data based on run 633.

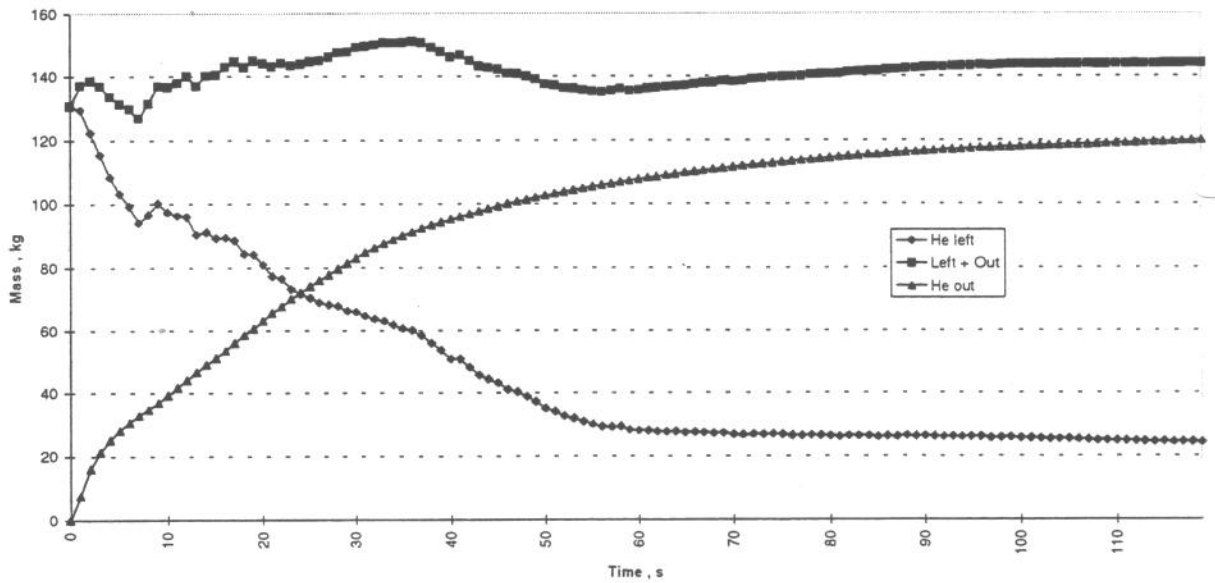


Fig.36. Helium mass balance during the string discharge, run 633: He_left - calculated with use of density as input data, he_out - integrated flow from figure 10.

11.Contents

1. Resistive transition of LHC magnets	1
2. The LHC helium recovery system	1
3. Lumped parameter approach to the recovery system	2
4. Enthalpy of helium leaving the cold mass after the quench	3
4.1. The prototype magnet string energy balance	3
4.2. Enthalpy flow of helium leaving the cold mass	9
4.3. Best estimation of the enthalpy of helium leaving the cold mass	12
5. Simulations of helium parameters in line D after a quench	13
5.1. Equilibrium parameters in line D, as a function of number of half-cells quenched	13
5.1.1. Influence of heat capacity of line D	14
5.1.2. Sensitivity of the results to enthalpy of the discharged helium	16
5.2. Dynamic characteristics of line D as a closed volume (no outflows)	17
5.3. LHC quench classification	21
5.4. Dynamic characteristics of line D with an outflow	22
6. Comparison of simulation results with the string experimental data	24
6.1. The string as a model of the LHC recovery system	24
6.2. Simulation of string quench, comparison with experimental data	24
7. Simulation of helium recovery in medium-pressure gas tanks	27
7.1. Convective heating on the vertical uninsulated line connecting line D with the MP tanks	27
7.2. Heat capacity of the medium-pressure gas tanks	29
7.3. Helium parameters in medium-pressure tanks during discharge of line D	30
8. Quench recovery	31
9. Conclusions	32
10. References	32
11. Appendixes	33
11.1. Appendix 1. Residual Resistance Ratio values of the outer layer coils of the string magnets.	33
11.2. Appendix 2. Helium density stratification during discharging the string through quench relief valve located close to MB3.	33